

REPUBLIQUE ALGERIENNE DEMOCRATIQUE ET POPULAIRE
MINISTRE DE L'ENSEIGNEMENT SUPERIEUR ET DE LA RECHERCHE
SCIENTIFIQUE

Université de Mohamed El-Bachir El-Ibrahimi - Bordj Bou Arreridj

Faculté des Sciences et de la technologie

Département d'Electronique

Mémoire

Présenté pour obtenir

LE DIPLOME DE MASTER

FILIERE : **Électronique**

Spécialité : Industries Électroniques

Par

- **MERMOUNE Faycel**
- **MERMOUNE Salah Eddine**

Intitulé

*Etude et commande d'un onduleur à qZ-source pour un générateur
photovoltaïque connecté*

Évalué le : 15/09/2021

Par la commission d'évaluation composée de :

<i>Nom & Prénom</i>	<i>Grade</i>	<i>Qualité</i>	<i>Etablissement</i>
<i>M. BOUKEZATA Boualem</i>	<i>MCB</i>	<i>Président</i>	<i>Univ-BBA</i>
<i>M. TALBI Billel</i>	<i>MCB</i>	<i>Encadreur</i>	<i>Univ-BBA</i>
<i>M. LAIB Abdelbaset</i>	<i>Doctorat</i>	<i>Co-encadreur</i>	<i>Univ-Sétif1</i>
<i>M. DJELLAL Djamel</i>	<i>MAA</i>	<i>Examineur</i>	<i>Univ-BBA</i>

Année Universitaire 2020/2021

* Conformément à :

- L'arrêté n°055 du 21 janvier 2021 Fixant dispositions exceptionnelles autorisées en matière d'organisation et gestion pédagogique, de l'évaluation et de la progression des étudiants, durant la période COVID-19 au titre de l'année universitaire 2020-2021 ;
- Procès-verbal de la réunion de l'équipe du domaine des Sciences et Technologies du mois de Mai 2021.

PEOPLE'S DEMOCRATIC REPUBLIC OF ALGERIA

MINISTRY OF HIGHER EDUCATION AND SCIENTIFIC RESEARCH

University of Mohamed El-Bachir El-Ibrahimi - Bordj Bou Arreridj

Faculty of Science and Technology

Department of Electronics

Presented to obtain

THE DIPLOMA OF MASTER

FIELD: Electronics

Speciality: Electronic Industries

By

- **MERMOUNE Faycel**
- **MERMOUNE Salah Eddine**

Entitled

*Study and control of qZ source inverter for grid-connected
photovoltaic system*

Evaluated on: 15/09/2021

By the evaluation committee composed of:

<i>Surname & First name</i>	<i>Grade</i>	<i>Quality</i>	<i>Establishment</i>
<i>M. BOUKEZATA Boualem</i>	<i>MCB</i>	<i>President</i>	<i>Univ-BBA</i>
<i>M. TALBI Billel</i>	<i>MCB</i>	<i>Supervisor</i>	<i>Univ-BBA</i>
<i>M. LAIB Abdelbaset</i>	<i>Doctorat</i>	<i>Co-supervisor</i>	<i>Univ-Sétif1</i>
<i>M. DJELLAL Djamel</i>	<i>MAA</i>	<i>Examiner</i>	<i>Univ-BBA</i>

Academic year 2020/2021

* Conformément à :

- L'arrêté n°055 du 21 janvier 2021 Fixant dispositions exceptionnelles autorisées en matière d'organisation et gestion pédagogique, de l'évaluation et de la progression des étudiants, durant la période COVID-19 au titre de l'année universitaire 2020-2021 ;
- Procès-verbal de la réunion de l'équipe du domaine des Sciences et Technologies du mois de Mai 2021.

Acknowledgements

In the name of ALLAH, the Most Gracious and the Most Merciful. Thanks to ALLAH who is the source of all the knowledge in this world, for the strengths and guidance in completing this thesis.

First of all, this work would not have been possible without the help and guidance of Dr. B. TALBI, we thank him for the quality of his exceptional supervision, for his patience, his availability during the preparation of this thesis, his moral support and encouragement. I would like to express my thanks to my co-supervisor, Dr. A. LAIB, for his comments and suggestions during the writing of this thesis.

We are aware that we have been honoured by the president of the jury and the examiner for agreeing to review this work.

Our thanks also go to all the teachers, the professors, our parents, our brothers, our sisters, our dear friends, for their help and their sacrifices.

Table of contents

List of figures.....	iv
List of tables.....	vi
List of acronyms.....	vii
Introduction general.....	1
Chapter I: Backgrounds on Grid-Connected Photovoltaic Systems	
I.1. INTRODUCTION	2
I.2. PHOTOVOLTAIC ENERGY.....	2
I.3. PHOTOVOLTAIC SYSTEMS	3
I.3.1. Stand-alone systems	4
I.3.2. Grid-connected systems	5
I.4. POWER ELECTRONICS INTERFACING TOPOLOGIES FOR GRID-CONNECTED PV SYSTEMS	6
I.4.1. Single-stage grid-connected systems	7
I.4.2. Two-stage grid-connected systems.....	7
I.5. CONTROL OBJECTIVES OF GRID-CONNECTED PV PHOTOVOLTAIC SYSTEMS.....	8
I.6. CONCLUSION	9
Chapter II: Modeling and Control of a Grid-Connected PV System using qZ Source Inverter	
II.1. INTRODUCTION.....	11
II.2 SYSTEM DESCRIPTION AND MODELLING.....	11
II.2.1. PV generator model	12
II.2.2. Quasi-Z source inverter model.....	13
II.3. SUGGESTED CONTROL SCHEME	19
II.3.1. MPPT algorithm	19
II.3.2. Model predictive current controller	21
II.3.3.1. Basic operating of model predictive control	22
II.3.3.2. Control algorithm.....	23
II.4. SIMULATION RESULTS	25

II.5. CONCLUSION.....	34
General Conclusion.....	35
References.....	34

List of figures

Figure	Title	Page
I.1	A typical PV system	4
I.2	Block diagram of a standalone PV system supplying a DC load	5
I.3	Block diagram of a standalone PV system supplying an AC load	5
I.4	Photovoltaic grid interfacing system technologies	7
I.5	Single stage grid-connected PV-system	8
I.6	Two-stage grid-connected PV-system	9
I.7	General control blocks (control objectives) of a grid-connected PV system	10
II.1	Studied single-stage grid-connected PV system configuration	12
II.2	Equivalent Electrical circuit of a photovoltaic cell	12
II.3	Three-phase QZ source inverter	14
II.4	Operating modes for QZ source inverter	15
II.5	Voltage vectors for qZSI	16
II.6	Suggested control scheme for studied grid-connected PV system	19
II.7	Power-Voltage characteristics of the PV operating points using P&O algorithm	20
II.8	P&O algorithm flowchart	21
II.9	Principle of Model Predictive Control	22
II.10	MPC algorithm for two steps to the future	24
II.11	MPC flowchart for qZSI	24
II.12	Schema block diagram of the developed simulation	25
II.13	Current-voltage (a) and power-voltage (b) characteristics of the PV array for different temperatures	26
II.14	Current-voltage (a) and power-voltage (b) characteristics of the PV array for different irradiance levels	27
II.15	Waveforms of: (a) PV power, (b) PV voltage and b) PV current array under fixed climatic conditions	27
II.16	Waveform of capacitor C_1 voltage under fixed climatic conditions	28
II.17	Waveform of inductor L_1 current under fixed climatic conditions	29
II.18	Waveforms of grid-injected three-phase currents under fixed climatic conditions	29
II.19	Grid-injected phase (a) current and voltage (i_{ga} & v_{ga})	30
II.20	FFT analysis of phase (a) output current under fixed climatic conditions	30
II.21	Waveform of PV power array during variation in irradiance level	31

II.22	Waveform of capacitor C_1 voltage during irradiation variation	32
II.23	Waveform of inductor L_1 current during irradiance variation	32
II.24	Waveforms of grid-injected three-phase currents during irradiance variation	33

List of tables

Table	Title	Page
II.1	PV module parameters	26
II.2	Electrical Parameters of the grid-connected PV system	26
II.3	Obtained THD under different irradiance levels	33

List of Acronyms

Acronym	Meaning
AC	Alternative Current
DPC	Direct Power Control
DC	Direct Current
GPV	Photovoltaic Generator
IncCon	Incremental Conductance
I-V	Current - Voltage
MPC	Model Predictive Control
MPP	Maximum Power Point
MPPT	Maximum Power Point Tracking
P-V	Power - Voltage
P&O	Perturb and Observe
PI	Proportional-integral
PID	Proportional-integral-derivative
PLL	Phase-Locked Loop
PV	PhotoVoltaic
THD	Total Harmonic Distortion
qZSI	quasi-Z Source Inverter

General Introduction

Nowadays, the world depends heavily on non-renewable energy sources such as coal, oil and natural gas. Meanwhile, energy production is a major challenge in the coming years due to the increasing energy needs, which leads to an increase the environmental pollution caused by previous sources. As a solution for this crisis, the world has begun to use another type of energy called renewable energies, for example, wind energy, solar energy, and biomass. Because it is characterized by unlimited sources and does not affect negatively the environment [1].

Among all renewable energy sources, solar photovoltaic (PV) energy is becoming increasingly competitive with conventional energy sources. Where, the grid-connected PV energy is one of the fastest growing and most promising renewable energy sources in the world [2].

Although the core of a PV system is the PV cell (also known as a PV generator), power electronics plays a fundamental role as an enabling technology for an efficient PV system control and interface to transfer the generated PV power to the grid. The functions of the power converter stage of a PV system include maximum power point tracking (MPPT), DC-AC power conversion, grid synchronization, grid code compliance (power quality), active and reactive power control [2].

The purpose of this work is to design an effective control scheme for grid-connected photovoltaic system using quasi-Z source inverter (qZSI). The qZSI provides a cheaper, simpler, and one stage approach for PV arrays.

This work is organized into two chapters:

- The first chapter is dedicated to PV systems, particularly grid connected PV systems, as well power electronics interfacing topologies for these systems and the control objectives of them.
- In the second chapter, we will be modeling and controlling grid-connected PV system based on qZSI using model predictive control technique.

Finally, a general conclusion and perspectives conclude this work.

Chapter I:

Backgrounds on Grid- Connected Photovoltaic Systems

I.1. Introduction

Recently, PV technology has been one of the promising renewable energy due to its ability to produce electricity without any pollution to the environment. PV systems are considered one of the most efficient and well-accepted renewable energy sources because of their suitability in distributed generation, mobile applications, transportation, and satellite systems. In addition, the PV systems price has decreased steadily over the years especially for the grid-connected PV-system, given the strong government support by most of the developed countries [1].

In this chapter, a short review on grid connected PV systems is offered to explain PV energy and present PV systems with their categories. In addition, power electronics interfacing topologies for grid connected PV systems and the control objectives of these systems are described respectively.

I.2. Photovoltaic energy

Every day, the sun provides energy to Earth. Human can use this free energy through a technology called photovoltaics. The word photovoltaics (PV) was first mentioned around 1890, and it comes from the Greek words: photo, ‘phos,’ meaning light, and ‘volt,’ which refers to electricity, describing exactly the photovoltaic phenomenon where you can directly convert light into electricity [2].

PV energy is a clean, renewable source of energy that uses solar radiation to produce electricity. It is based on the so-called photoelectric effect, by which certain materials can assimilate photons (light particles) and discharge electrons producing an electric current. For

Principally, PV systems can be divided into two categories according to their application:

- Stand-alone systems.
- Grid-connected systems.

I.3.1. Stand-alone systems

Also known as off-grid PV power system, usually requires a storage battery, this type generally operates independently of the utility grid, designed and sized to supply certain DC and/or AC electrical loads.

For DC load application, PV systems utilize single-stage DC-DC power converter, which plays a major role in changing the PV voltage or current level for tracking the maximum power point (MPP). For AC load application, a two-stage topology along with battery banks connected between the two stages is used. In the first stage, a DC-DC converter is used to boost the PV voltage and track the MPP. In the second stage, the DC-AC inverter is utilized to convert the DC power to AC power and improve the AC power quality. In case of PV application with a critical load, battery banks are used to fix the inverter DC voltage and enhance or supply the required load power [2].

Figures I.2 and I.3 show, respectively, the block diagram of the standalone PV system for DC and AC load.

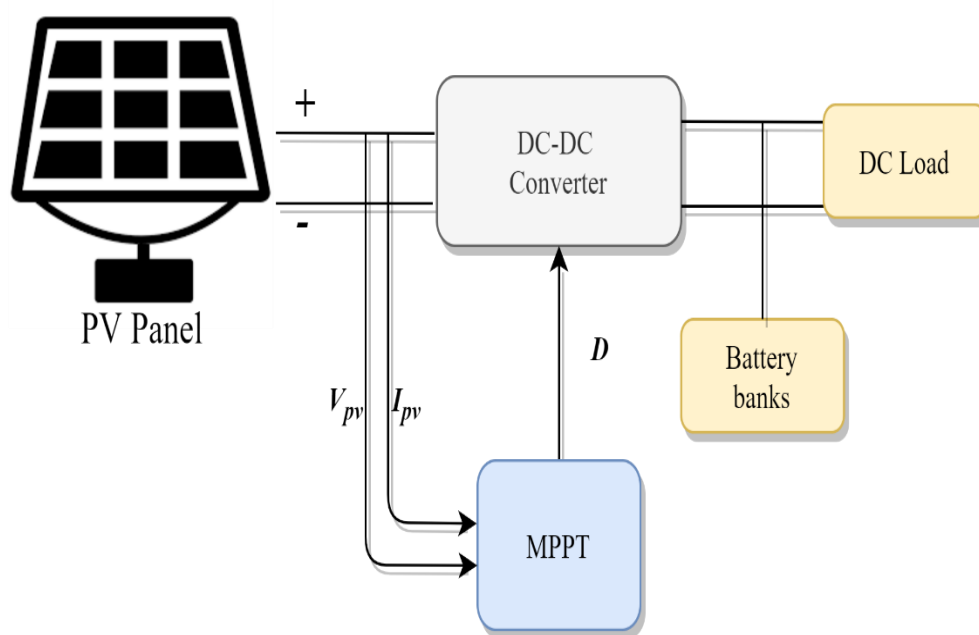


Figure I.2: Block diagram of a standalone PV system supplying a DC load.

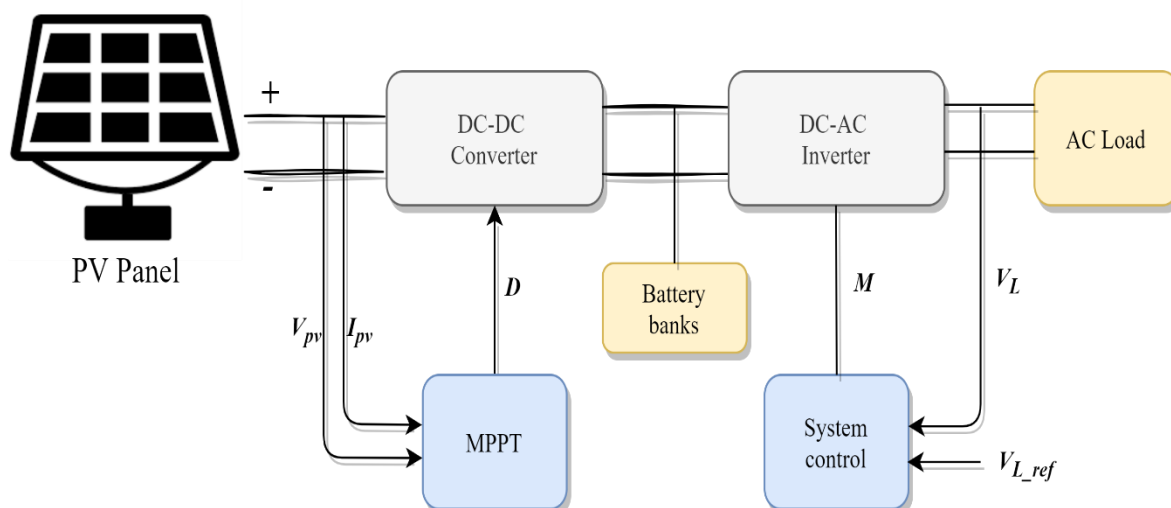


Figure I.3. Block diagram of a standalone PV system supplying an AC load.

I.3.2. Grid-connected systems

In order to inject the power generated by PV modules into the grid, it must be converted first from DC power to AC power. So, a power electronics inverter is employed. In addition to the converting capability, the inverter is used for the MPPT (maximum power point tracking). Also, a DC-DC converter could be used to boost the PV output voltage and track the MPP. There are different inverter configurations:

- Centralized technology.
- String technology.
- Multi-string technology.
- AC-module technology.

Figure I.4 shows the grid-connected PV system technologies. Centralized inverter technology is considered the first PV grid-connected configuration. PV strings (a number of PV modules connected in series) are connected in parallel in order to obtain a PV array with the desired output power and DC voltage level. The PV array output is connected to a single DC to AC inverter. In this configuration, PV maximum power is delivered into the grid with high efficiency, small size, and low cost. Although, to fulfil grid requirements, such topology requires either a step-up transformer, which reduces the system efficiency and increases cost, or a PV array with a high DC voltage. A high voltage PV system suffers from hotspots (where a PV module with lower radiation behaves as a load) during partial shading and increased leakage current between the PV panel. Furthermore, the parallel connected PV strings could

have different optimum voltages, resulting in multiple peaks on the PV array characteristic curve. To improve MPPT during partial shading or string optimum voltage mismatch, string technology is used, where each PV string is connected to an inverter with its own MPPT. This configuration has few drawbacks, it requires a large number of components and has high installation costs. The multi-string technology is similar to string technology. The difference is that a DC-DC converter is installed on each PV string where the outputs of each DC-DC converter are connected to a single DC-AC inverter. The added DC-DC converter on each string is employed to track the MPP and avoids having a large DC voltage PV module, this technology is expensive because each string has its own converter. In AC-module technology, each PV module is connected to a different inverter, where the MPP from each module is extracted separately. This technology is recommended when PV modules with different power rating are used and it is considered the most expensive [3].

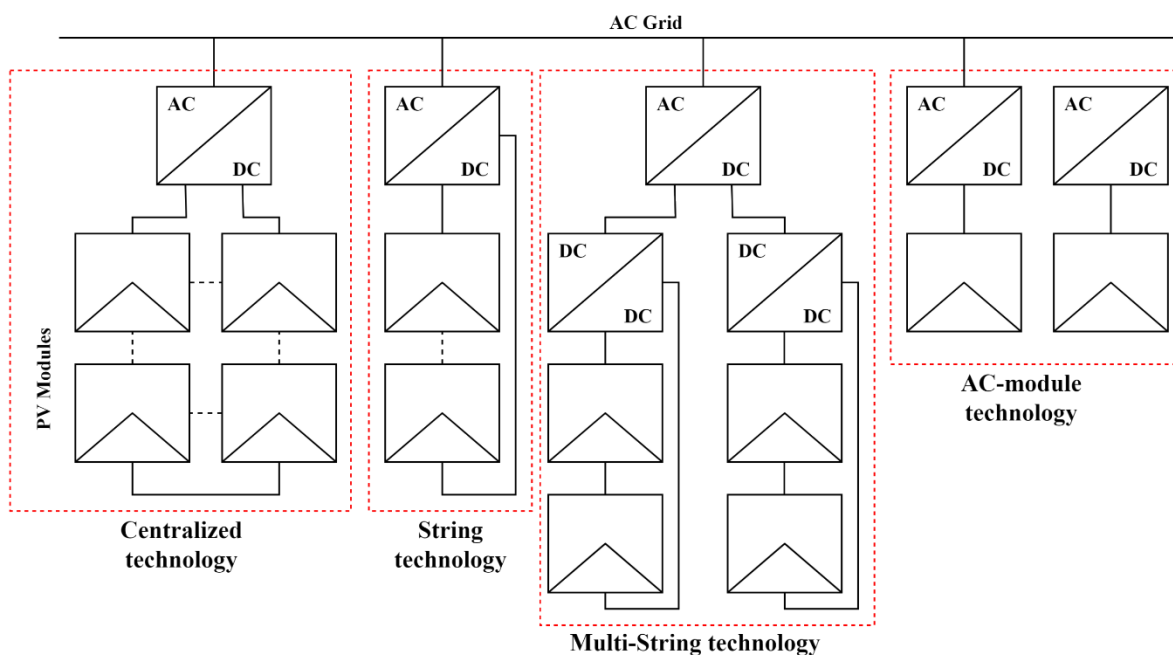


Figure I.4: Photovoltaic grid interfacing system technologies.

I.4. Power electronics interfacing topologies for grid-connected PV systems

Given to the development of PV technologies, applications of PV in grid-connected situations have grown rapidly and there has been a progress in the new power inverters topologies the last few years. The main research efforts have concentrated on the highest possible efficiency, power density, and reliability of the converter to further increase the overall performance of the PV installation. In this part, both of single stage and two stage grid connected PV systems are introduced.

I.4.1. Single-stage grid-connected systems

A single-stage grid-connected system is illustrated in Figure I.5. In order to track the MPP and interface the PV system to the grid, the PV system utilizes a single conversion unit (DC-AC power inverter). In such topology, PV maximum power is delivered into the grid with high efficiency, small size, and low cost. However, to fulfil grid requirements, this topology requires either a step-up transformer, which reduces the system efficiency and increases cost, or a PV array with a high DC voltage. High voltage systems suffer from hotspots during partial shading and increased leakage current between the panel, as described in section I.3.2. Furthermore, it is complicated to control the inverter because the control objectives such as MPPT, power factor correction and harmonic reduction. Different types of DC-AC inverters have been applied to enhance and regulate the performance, such as two-level and multilevel voltage source inverters and current source inverters [2].

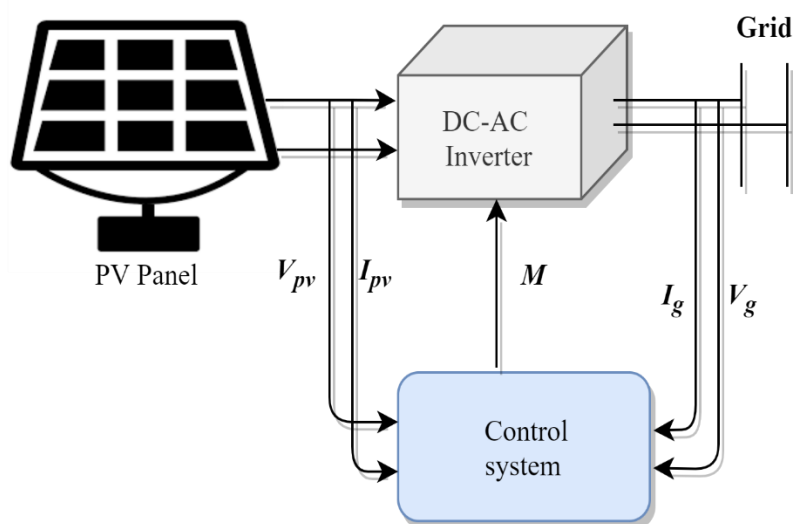


Figure I.5. Single stage grid-connected PV-system.

I.4.2. Two-stage grid-connected systems

A block diagram of two stage grid-connected PV-system is presented in Figure I.6. The first stage is normally a DC-DC converter for extracting maximum power from the PV panel, the second one is a DC-AC converter for delivering power to the grid, and each of them is controlled in purpose of reducing load current ripple and keeping the output voltage level at desired value. The advantages of the two-stage topology lie in the simplicity of designing the control scheme, since the control requirements are distributed between the two stages. Furthermore, a PV array with a high voltage output is not required because of the first

amplification stage. This topology suffers from higher power losses, larger footprint and higher cost than single-stage systems [2].

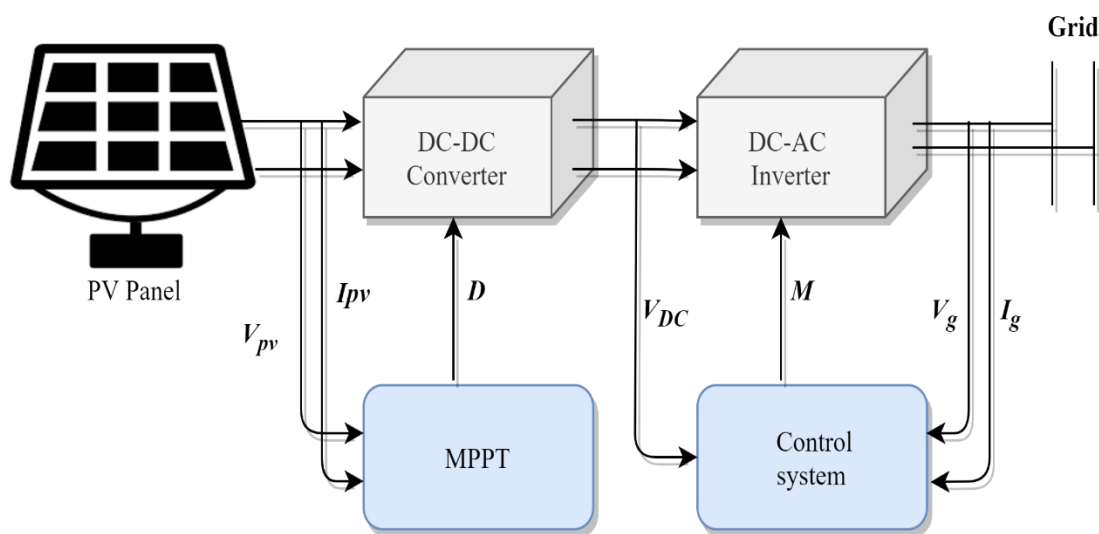


Figure I.6: Two-stage grid-connected PV-system.

I.5. Control objectives of grid-connected PV photovoltaic systems

As shown in Figure I.7, the control objectives of a grid-connected PV system can be divided into two major parts: PV-side control with the purpose to maximize the power from PV panels and (2) grid-side control performed on the PV inverters with the purpose of fulfilling the demands to the grid. In order to maximize the power, it is important to track the most extreme power point of the PV generator. PV system has a single operating point which can give maximum power to the load. This point is called the maximum power point (MPP). Hence, to function the PV generator at its greatest power point, distinctive algorithms can be utilized such as perturb and observe (P&O), Incremental Conductance (IncCon) which are very popular because of their simplicity and fast convergence. Also, there are other intelligent algorithms as fuzzy control, genetic algorithms, etc. But they have some drawbacks, including complex implementation and difficulties in initial point selection. On the other side, different control strategies are also applied in a closed-loop for a photovoltaic inverter to generate a gating pulse signal such as direct power control (DPC) and the reference current extraction methods. In the last methods, a PI controller is used to regulate the DC-link voltage and estimate the amplitude of the reference grid currents. It should be noted that the injected grid current is demanded to be synchronized with the grid voltage, different methods to extract the grid voltage information have been developed in recent studies like the zero-crossing method, the filtering of grid voltage

method, and the phase-locked loop (PLL) techniques, which give the best performance. PLL is a feedback control system used generate an output signal when the phase is related to the phase of input signal, only if frequency, voltage and phase are the same, it creates an output signal [4].

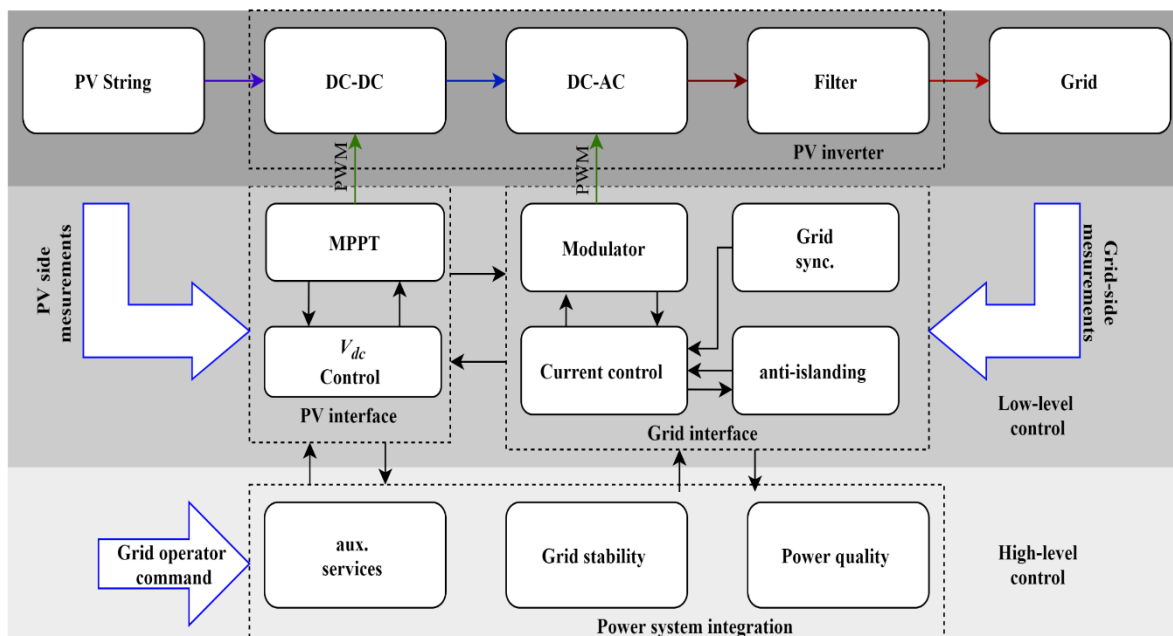


Figure I.7: General control blocks (control objectives) of a grid-connected PV system.

I.6. Conclusion

In this chapter, we discussed backgrounds on grid-connected PV systems. The PV systems were partitioned into two types, grid-connected and stand-alone PV systems. Since achieving higher conversion efficiency is always of intense interest in grid-connected PV systems, both the single-stage (without a DC–DC converter) and the two-stage (with a DC–DC converter) PV topologies have been described. Finally, the general control objectives for grid-connected PV systems are presented. The next chapter will focus on the modeling and control of a grid-connected PV system.

Chapter II:

Modeling and Control of a Grid-Connected PV System using qZ Source Inverter

II.1. Introduction

The use of advanced power conversion systems and sophisticated controllers presents an increasing interest because it improves the energy production and the quality of operation of grid-connected PV systems. As discussed in the previous chapter, a transformerless single-stage grid-connected PV system has higher efficiency and lower weight and size; but, by removing the DC-DC boost converter between the PV generator and the DC-AC voltage source inverter, the PV array with a high DC voltage is required to fulfil grid requirements. The quasi-Z-source inverter (qZSI) can overcome this issue due to the following reasons:

- The DC input current of qZSI is continuous which is important for PV application.
- The qZSI voltage boosting capability allows a low-voltage PV array to be grid interfaced without the need of a transformer or an additional boost stage.

In this context, a single-stage three-phase grid-connected PV system based on a qZSI is presented in this chapter. In addition, an effective control scheme based on advanced technique ‘‘ Model predictive control ‘‘ for the presented grid-connected PV system is developed.

II.2 SYSTEM DESCRIPTION AND MODELLING

Following the discussion in the previous chapter, a typical configuration of a single-stage grid-connected PV system, shown in Figure II.1, is a promising solution for an effective, economic and robust grid-connected PV system. The system includes a PV array, a passive

filter (capacitor), which is used to reduce the current and voltage ripple (and hence power), and a quasi-Z source inverter connected to the grid through passive RL filter.

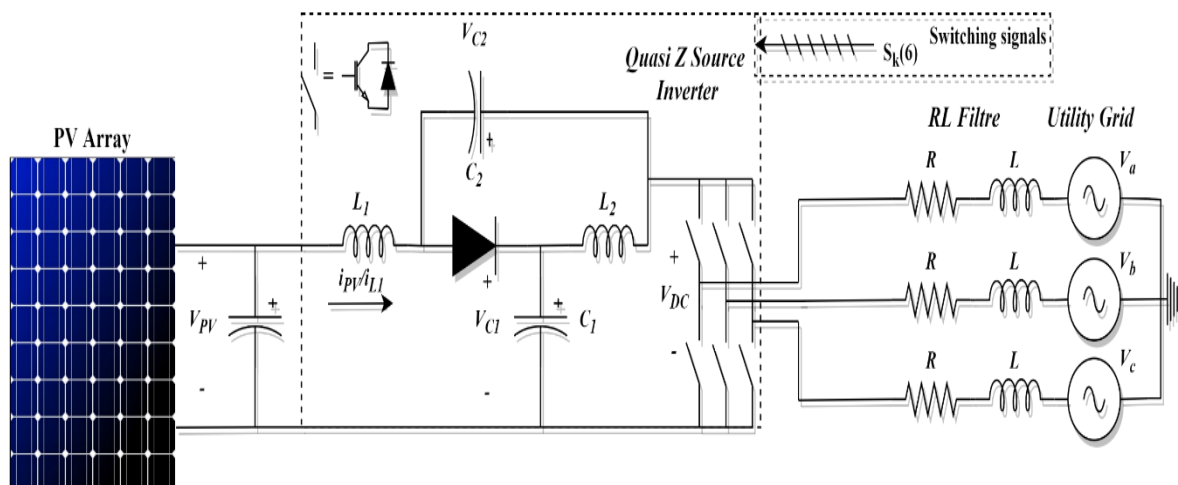


Figure II.1: Studied single-stage grid-connected PV system configuration.

II.2.1. PV generator model

PV cell models have long been a source for the description of PV cell behavior. The most common model used to predict the energy production in a PV cell modeling is the single diode circuit model shown in Figure II.2. A photocurrent source I_{ph} in parallel with a diode, a series resistance R_s and a shunt resistance R_{sh} .

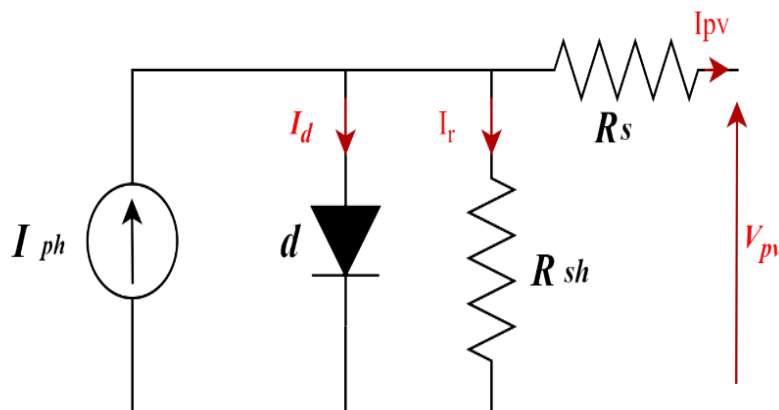


Figure II.2. Equivalent Electrical circuit of a photovoltaic cell.

This model includes a current source I_{ph} , which depends on solar radiation and cell temperature, a diode which the inverse saturation current I_0 depends mainly on the operating temperature, a series resistance R_s and a shunt resistance R_{sh} , taking into account the resistive losses. The current–voltage relationship of a PV cell is given by:

$$I_{pv} = I_{ph} - I_d - I_r = I_{ph} - I_0 \left[e^{\frac{q(V_{pv} + R_s I_{pv})}{akt}} - 1 \right] - \frac{V_{pv} + R_s I_{pv}}{R_{sh}} \quad (\text{II.1})$$

where:

I_{pv} : is the cell output current (A).

I_d : is the diode current (A).

I_r : is the derived current by the shunt resistance (A).

I_{ph} : is the cell photocurrent (A).

I_0 : is the reverse saturation current of the diode (A).

R_{sh} : is the cell shunt parasitic resistance (Ω).

R_s : is the cell series parasitic resistance (Ω).

V_{pv} : is the cell output voltage (V).

q : is the electronic charge ($1.6 * 10^{-19}$ J).

k : is the Boltzmann constant ($1.38 * 10^{-23}$ J/K).

t : is the absolute temperature (K).

a : is the diode ideality factor.

PV cells are combined in series and parallel connection to form larger units called PV modules, which are further interconnected in a series-parallel configuration created PV array. A PV array, which consists of n_s PV cells in series and n_p PV cells in parallel [5], can be modeled by:

$$I_{pv} = n_p I_{ph} - n_p I_0 \left[e^{\frac{q(n_s V_{pv} + (\frac{n_s}{n_p}) R_s I_{pv})}{akt n_s}} - 1 \right] - \frac{n_s V_{pv} + (\frac{n_s}{n_p}) R_s I_{pv}}{(\frac{n_s}{n_p}) R_{sh}} \quad (\text{II.2})$$

where:

I_{pv} : is the array output current (A).

V_{pv} : is the array output voltage (V).

II.2.2. Quasi-Z source inverter model

Recently, the step-up impedance source inverters have been presented as a competitive alternative to overcome the voltage limitation of the traditional inverter. These inverters do not convert a DC signal into an AC signal only; also raise the voltage of the source to a higher level. The qZSI topology was first suggested to overcome the discontinuous input current problem in

the original Z-source inverter by providing continuous input current, which leads to a better interface for DC sources such as PV cells. The qZSI network uses a combination of two inductors and two capacitors and a diode as shown in Figure II.3. Since the switching frequency is much higher than that of the source, the inductors and capacitors should be low [6].

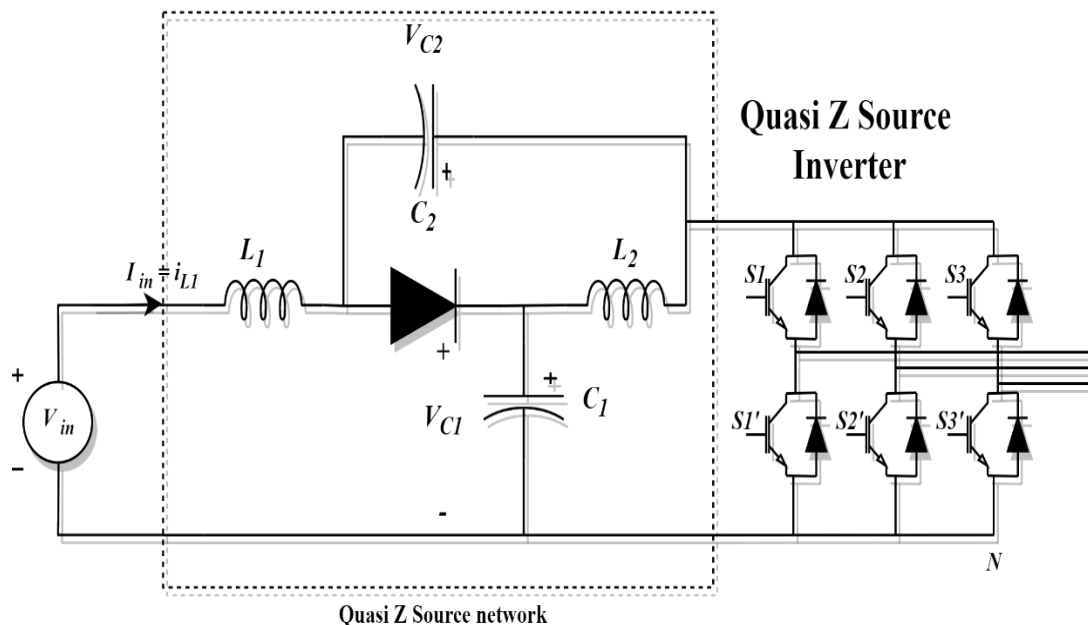


Figure II.3: Three-phase QZ source inverter.

The qZSI has three different operating modes: active state, null state and shoot-through state as illustrated in Figure II.4. During the active state, shown in Figure II.4(a), the inverter is controlled in the same way as a conventional voltage source inverter only without dead time. On the DC-input side, during the active state the diode will turn ON and capacitor C_1 will discharge through inductor L_2 . In the null state shown in Figure II.4(b), all three top switches or bottom switches of the inverter are turned ON which disconnects the inverter output from the input and providing a freewheeling path for the load current. Inductor L_2 current will flow through capacitor C_2 and the diode. Moreover, the current flowing in inductor L_1 will charge capacitor C_1 via the diode. Finally, as shown in Figure II.4(c), the shoot-through state occurs when both high-side and low-side switches in the same phase leg are turned on simultaneously. During this state, there can be one, two, or all three phases of the inverter short circuited. The inductor L_2 will connect to the capacitor C_1 and the source will connect to the capacitor C_2 through the inductor L_1 . Capacitor C_1 transfers the energy to the inductor L_2 , and inductor L_1 will be charged from the source and capacitor C_2 .

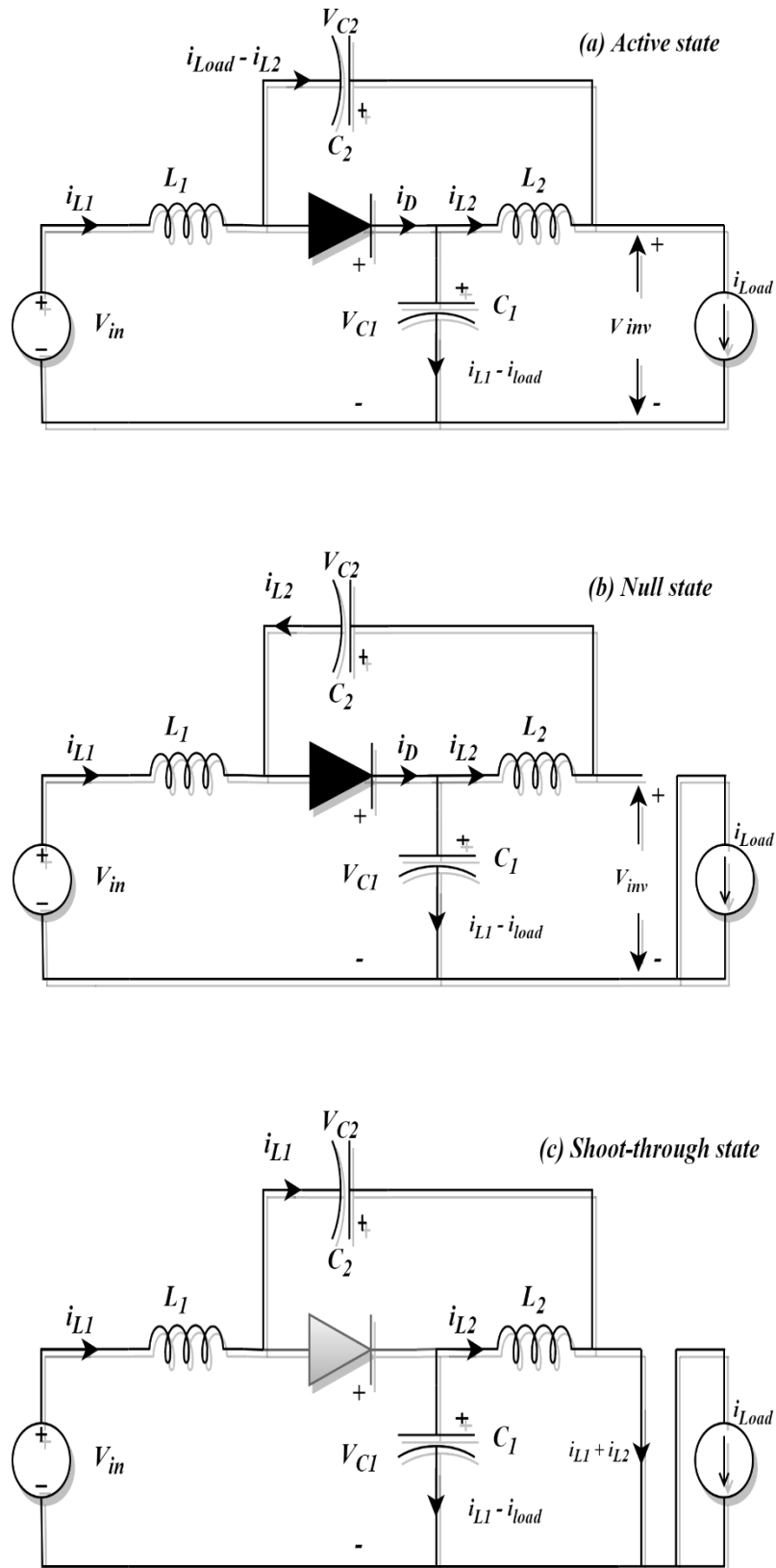


Figure II.4: Operating modes for QZ source inverter.

The three-phase inverter has a total of fifteen valid switch configurations. Figure II.5 shows the vector diagram for two phases (α, β) where the fifteen states create as six active-states vectors (V_1, V_2, \dots, V_6), two null state vectors (V_0), and seven shoot-through state vectors (V_7). Many of these states are redundant as they produce the same output voltage vector: the null states and the shoot-through states can be simplified into one switch configuration for each. This reduces the controller computation time since less switching configurations need to be evaluated for the selection of the optimal voltage vector [7].

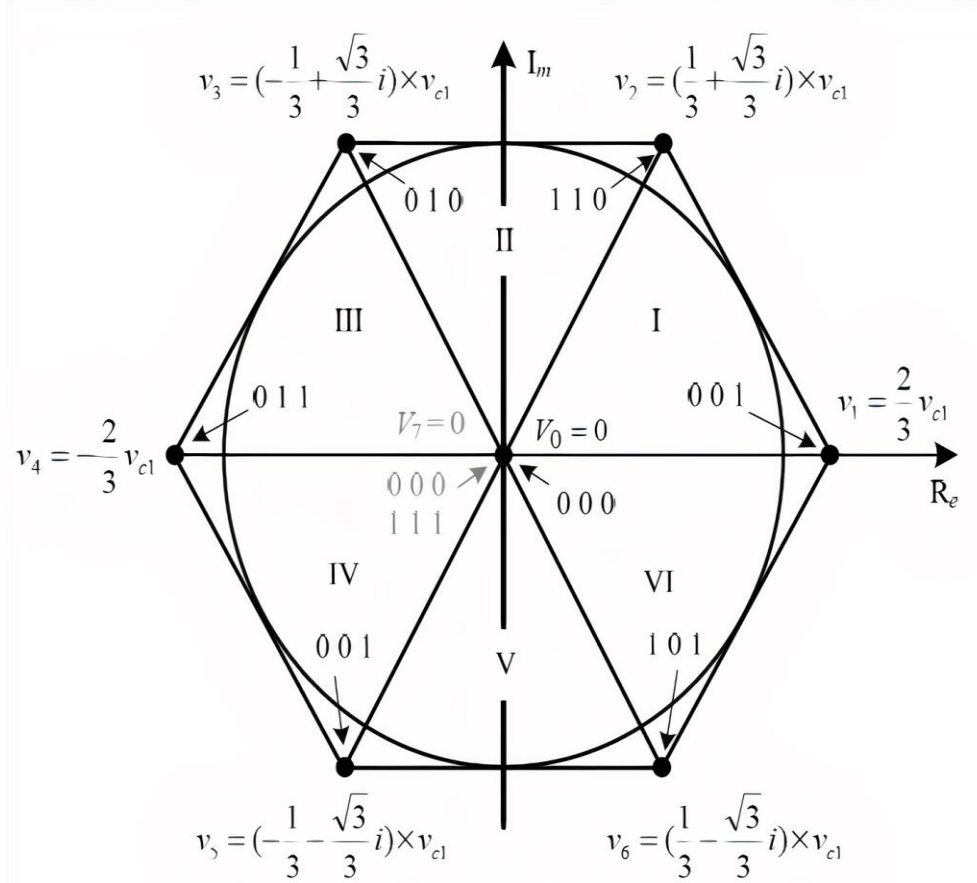


Figure II.5: Voltage vectors for qZSI.

The output voltages can be represented in terms of the space vector as following:

$$V_{out} = \frac{2}{3}(V_{an} + a \times V_{bn} + a^2 V_{cn}) \quad (II.3)$$

where $a = -\frac{1}{2} + j\frac{\sqrt{3}}{2}$, and V_{an}, V_{bn} and V_{cn} are the phase leg simple voltages.

According to Figure II. 1, the output voltage vector of the qZSI can be described as follows:

$$V_{out} = L \frac{di_{out}}{dt} + R \cdot i_{out}(\alpha, \beta) + v_g(\alpha, \beta) \quad (II.4)$$

where L is the filter inductance, i_{out} is the output current vector of the qZSI, R is the filter resistance and v_g is the grid voltage vector. So, the voltage of the filter inductance is determined by:

$$L \frac{di_{out}}{dt} = V_{out} - R \cdot i_{out}(\alpha, \beta) - v_g(\alpha, \beta) \quad (II.5)$$

All three operational states of the qZSI will be considered: active, null, and shoot-through, in order to find the output current, the current through inductor L_1 .

a) Active state:

From figure II.4 (a), capacitor C_1 current and inductor L_1 voltage are given by the following equations:

$$C1 \frac{dV_{c1}}{dt} = i_{L1} - i_{inv} \quad (II.6)$$

$$L1 \frac{di_{L1}}{dt} = V_{in} - V_{C1} \quad (II.7)$$

Where i_{inv} is the input current to the three-phase inverter which is equal to i_{out} in this case (instantaneously).

b) Null state:

From figure II.4(b), capacitor C_1 current and inductor L_1 voltage can be expressed as:

$$C1 \frac{dV_{c1}}{dt} = i_{L1} \quad (II.8)$$

$$L1 \frac{di_{L1}}{dt} = V_{in} - V_{C1} \quad (II.9)$$

c) Shoot-through state:

From figure II.4(c), the capacitor current and the inductor voltage are:

$$C1 \frac{dV_{c1}}{dt} = i_{L1} \quad (II.10)$$

$$L1 \frac{di_{L1}}{dt} = V_{C1} \quad (II.11)$$

Using the Euler method with sampling time T_s :

$$\begin{aligned} \frac{di_{out}}{dt} &\approx \frac{i_{out}(t) - i_{out}(t - T_s)}{T_s} \\ \frac{dV_{C1}}{dt} &\approx \frac{V_{C1}(t) - V_{C1}(t - T_s)}{T_s} \\ \frac{di_{L1}}{dt} &\approx \frac{i_{L1}(t) - i_{L1}(t - T_s)}{T_s} \end{aligned} \quad (II.12)$$

Considering the previous approximation:

- From equation (II.5):

$$i_{out}(t)(\alpha, \beta) = i_{out}(t - T_s)(\alpha, \beta) + \frac{T_s}{L} [V_{out}(t) - Ri_{out}(t)(\alpha, \beta) - v_g(t)(\alpha, \beta)] \quad (II.13)$$

From the instant t to $t+T_s$, the predicted future output current expression will be:

$$i_{out}(t + T_s)(\alpha, \beta) = \left(1 + \frac{R}{L}\right) T_s i_{out}(t)(\alpha, \beta) + \frac{T_s}{L} (V_{out}(t + T_s) - v_g(t)(\alpha, \beta)) \quad (II.14)$$

$i_{out}(t + T_s)$ is the output space vector for qZSI, which can be selectively generated through switches control.

- The expressions for the inductor L_1 current in each mode of operation for qZSI:
 - a) *Active and null state*

$$i_{L1}(t) = \frac{L_1 i_{L1}(t - T_s) + T_s (V_{in}(t) - V_{C1}(t))}{L_1} \quad (II.15)$$

So, the inductor predicted future equation is:

$$i_{L1}(t + T_s) = \frac{L_1 i_{L1}(t) + T_s (V_{out}(t + T_s) - V_{C1}(t + T_s))}{L_1} \quad (II.16)$$

Because the change in capacitor voltage is considerably smaller, the predictive value of the capacitor voltage can be considered equal to the present value. Therefore, the equation (II.16) can be rewritten as:

$$i_{L1}(t + T_s) = \frac{L_1 i_{L1}(t) + T_s (V_{out}(t + T_s) - V_{C1}(t))}{L_1} \quad (II.17)$$

- b) *Shoot-through state*

$$i_{L1}(t) = \frac{L_1 i_{L1}(t - T_s) + T_s V_{C1}(t)}{L_1} \quad (II.18)$$

Considering what we mentioned before about the small changing of the capacitor voltage, the predictive expression of the inductor current is:

$$i_{L1}(t + T_s) = \frac{L_1 i_{L1}(t) + T_s V_{C1}(t)}{L_1} \quad (II.19)$$

II.3. Suggested control scheme

Figure II.6 illustrates the complete control scheme used to control the system in Figure II.1. Where the MPPT is utilized to track the maximum power from the PV array using a method called P&O (Perturbation and observation). Phase Locked Loop (PLL) block ensures that both grid current and voltage are synchronized, and the PI controller regulates the capacitor C_1 voltage and estimate the amplitude of the reference grid currents. MPC algorithm controls the qZSI by providing proper switching signals each sample time T_s , based on the future prediction of the inductance L_1 current i_{L1} and the output current i_{out} .

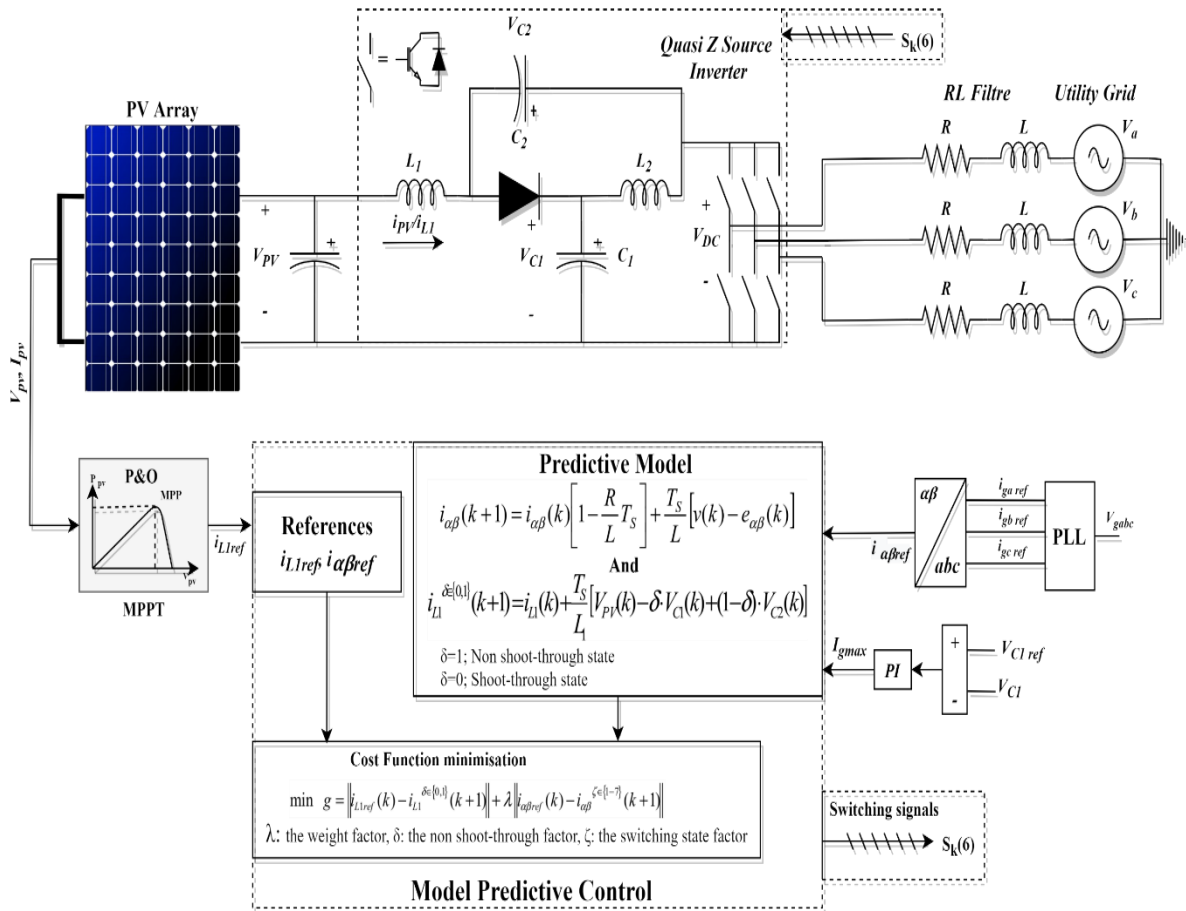


Figure II.6: Suggested control scheme for studied grid-connected PV system.

II.3.1. MPPT algorithm

The output power of PV arrays is always changing with weather conditions, which mean solar irradiation and atmospheric temperature. It is important to operate PV energy conversion systems near the maximum power point to increase the output efficiency of PV arrays. Some MPPT techniques are available such as fractional open-circuit voltage and short-circuit current

methods, Incremental conductance algorithm ...etc. In this project, we used perturbation and observation technique, a simple algorithm that operates by periodically perturbing (i.e. incrementing or decrementing) the array terminal current or voltage and comparing the PV output power with that of the previous perturbation cycle. If the power is increasing, the perturbation will continue in the same direction in the next cycle, otherwise the perturbation direction will be reversed. This means the array terminal current or voltage is perturbed every MPPT cycle until the MPP is reached. When the perturb step is large, the tracking is quick and the power oscillations are significant. On the opposite, when the perturb step is small, slower tracking is accomplished with decreased power oscillations. The P&O algorithm will oscillate around the MPP resulting in a loss of PV power, especially in cases of constant or slowly varying atmospheric conditions. This problem can be solved by decreasing the perturbation step or improving the logic of the P&O algorithm to compare the parameters of two preceding cycles in order to check when the P&O is reached, and bypass the perturbation stage. The basic process of the P&O algorithm is shown in Figure II.7.

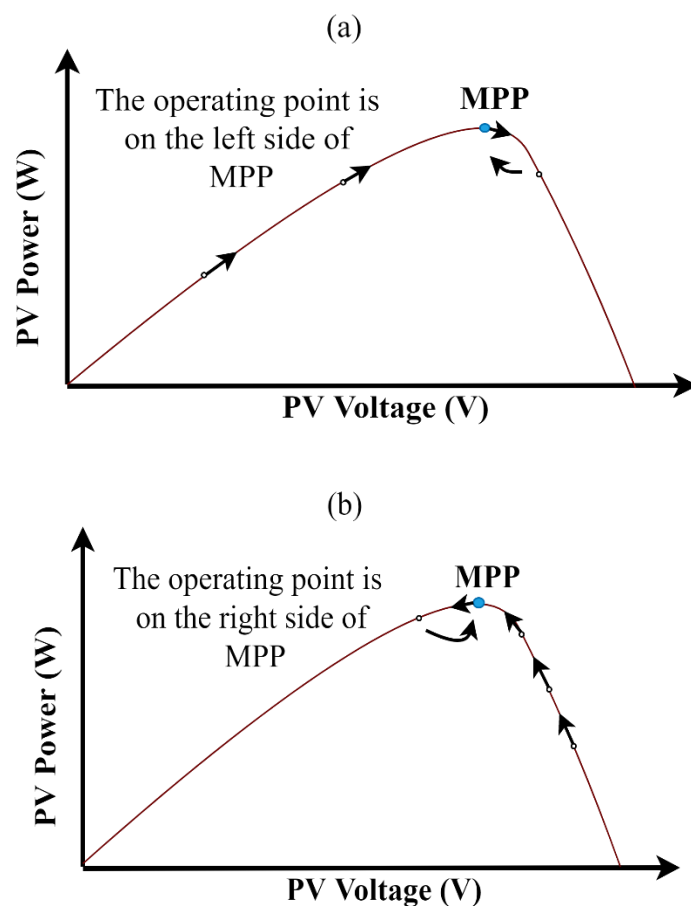


Figure II.7: Power-Voltage characteristics of the PV operating points using P&O algorithm.

The flowchart of the used P&O algorithm in this work is presented in Figure II.8. It considers current perturbation instead of voltage or duty cycle perturbation to speed up the tracking performance [8].

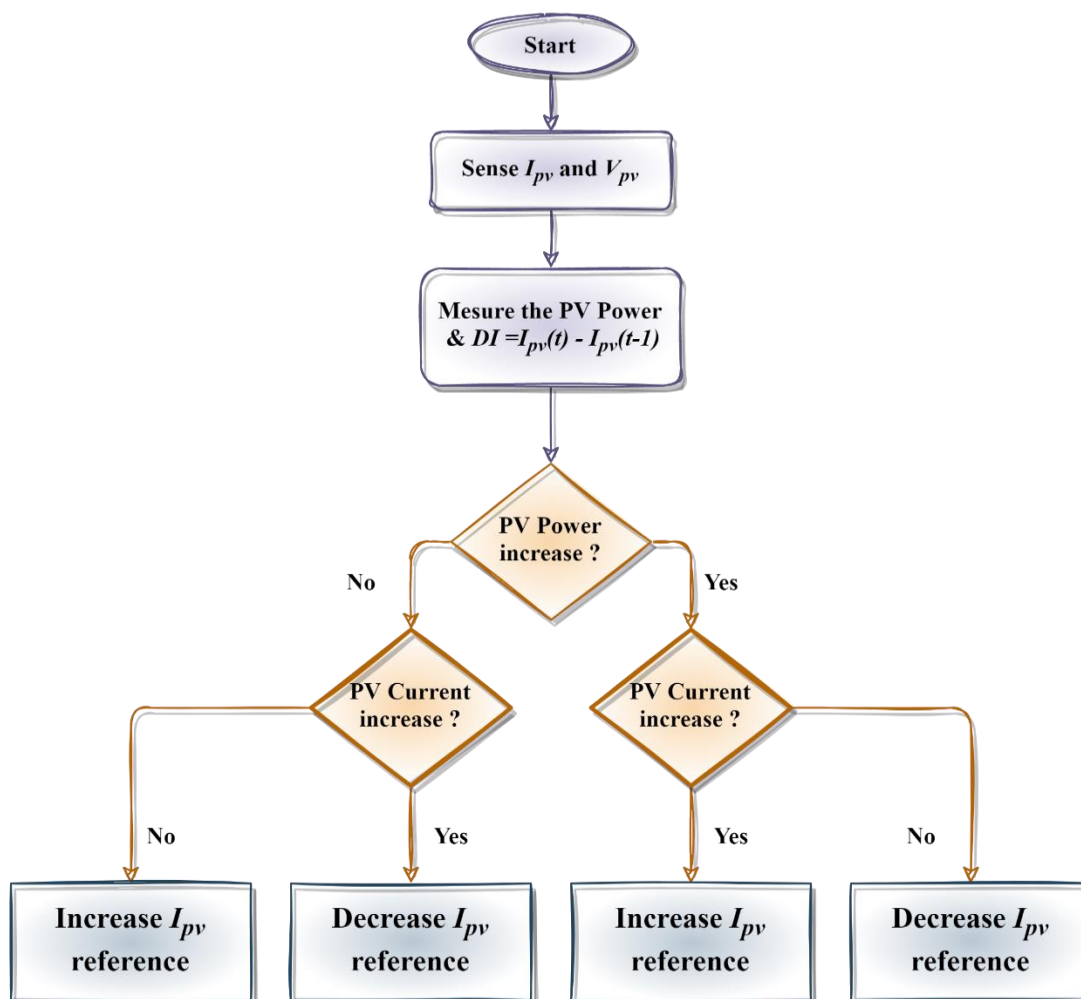


Figure II.8: P&O algorithm flowchart.

II.3.2. Model predictive current controller

Among the advanced control methods that's more progressed than standard PID-control, MPC (Model predictive control) is one that has been effectively utilized in industrial applications. In spite of the fact that the thoughts of MPC were created within the 1960s as an application of optimal control theory, industrial intrigued in these thoughts begun within the late 1970s. Early applications of the ideas of MPC in power electronics considered high-power systems with low switching frequency; the use of higher switching frequencies was not conceivable at that time due to the expansive calculation time required for the control algorithm. However, with the advancement of fast and powerful microprocessors, interest within the application of MPC in power electronics has expanded significantly over the final decade. MPC

describes a wide family of controllers not a particular control technique. The common components of this kind of controllers are that they use a model of the system to anticipate long term behavior of the variables until a predefined horizon in time, and selection of the optimal process by minimizing a cost function.

The MPC procedure is based on the truth that as it were a limited number of conceivable switching states can be produced by a static power converter and that models of the system can be utilized to foresee the behavior of the variables for each switching state. A selection criterion must be defined for the determination of the suitable switching state to be applied, this measure comprises of a cost function that will be assessed for the predicted values of the variables to be controlled, calculating of each possible switching state for the Prediction of the future value of these variables and then selecting the state that minimizes the cost function. This structure has a few critical advantages:

- Concepts are exceptionally instinctive and understandable.
- It can be connected to variety of systems.
- The multivariable case can be considered easily.
- Simple consideration of non-linearity within the model.
- Easy implementation of the resulting controller.

However, compared to classic controllers, it has a larger number of calculations, and the quality of the model has a direct impact on the quality of the resulting controller.

II.3.3.1. Basic operating of model predictive control

The principle of MPC is summarized in Figure II.9.

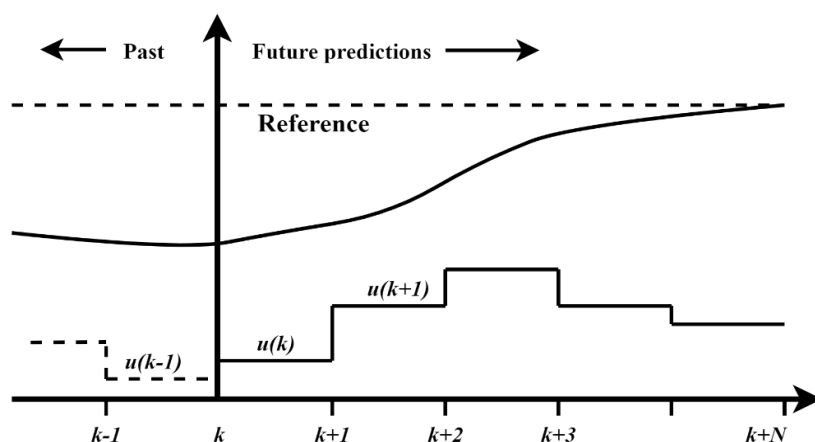


Figure II.9: Principle of Model Predictive Control.

Using the system model and the available measurements, the future values of the states of the system variables are predicted until a predefined horizon in time $k + N$. By minimizing the cost function, the sequence of optimal actuation is calculated and the first element of this sequence is applied. This entire process is repeated for each inspecting instant considering the new measured data [8].

II.3.3.2. Control algorithm

The MPC cost function used in this work is comprised of two weighted cost functions representing the AC output current, and inductor L_1 current. The output current cost function is defined as:

$$g_i = |i_{\alpha}^*(t + T_s) - i_{\alpha}(t + T_s)| + |i_{\beta}^*(t + T_s) - i_{\beta}(t + T_s)| \quad (\text{II.20})$$

where $i_{\alpha}^*(t+T_s)$, $i_{\beta}^*(t+T_s)$ are the real and imaginary parts of the future reference output current, and $i_{\alpha}(t+T_s)$, $i_{\beta}(t+T_s)$ are the real and imaginary components of the predicted load current. Furthermore, the cost function of the inductor L_1 current is defined as:

$$g_{iL} = |i_L^*(t + T_s) - i_L(t + T_s)| \quad (\text{II.21})$$

where $i_L^*(t+T_s)$, $i_L(t+T_s)$ are the reference and predicted inductor current, respectively. The complete cost function incorporates the previous functions into to one:

$$g = \lambda_i g_i + \lambda_{iL} g_{iL} \quad (\text{II.22})$$

where λ_i, λ_{iL} are respectively the weighting factors for output current and inductor L_1 current.

For the future inductor L_1 current, there are two prediction values which can be calculated from equations (II.17), and (II.19) as shown in Figure II.11 (one in active state and one in shoot-through state). The optimal point for the future inductor current is $i_{L1}^{p1}(2)$ which minimize the error. Then, the optimizer will choose the overall optimal state according to equation (II.22), a proper switching state will be chosen depending on this selection. Similarly for the next instant $t + 2T_s$, the controller will calculate the future points for the variables and the optimizer will choose the optimal points which is the nearest point to the reference [7].

The same process for the prediction of the AC output current $i_{out}(t)$, the optimizer chooses the optimal one of eight prediction states ($i_{\alpha}^{p1}(1)$ to $i_{\alpha}^{p1}(8)$) calculate from equation (II.14) which minimizes the cost function.

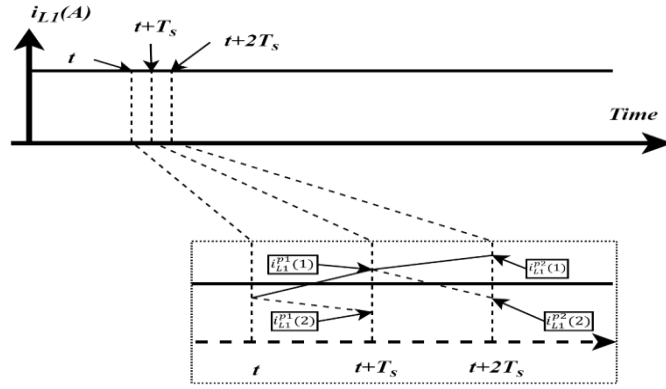


Figure II.10: MPC algorithm for two steps to the future.

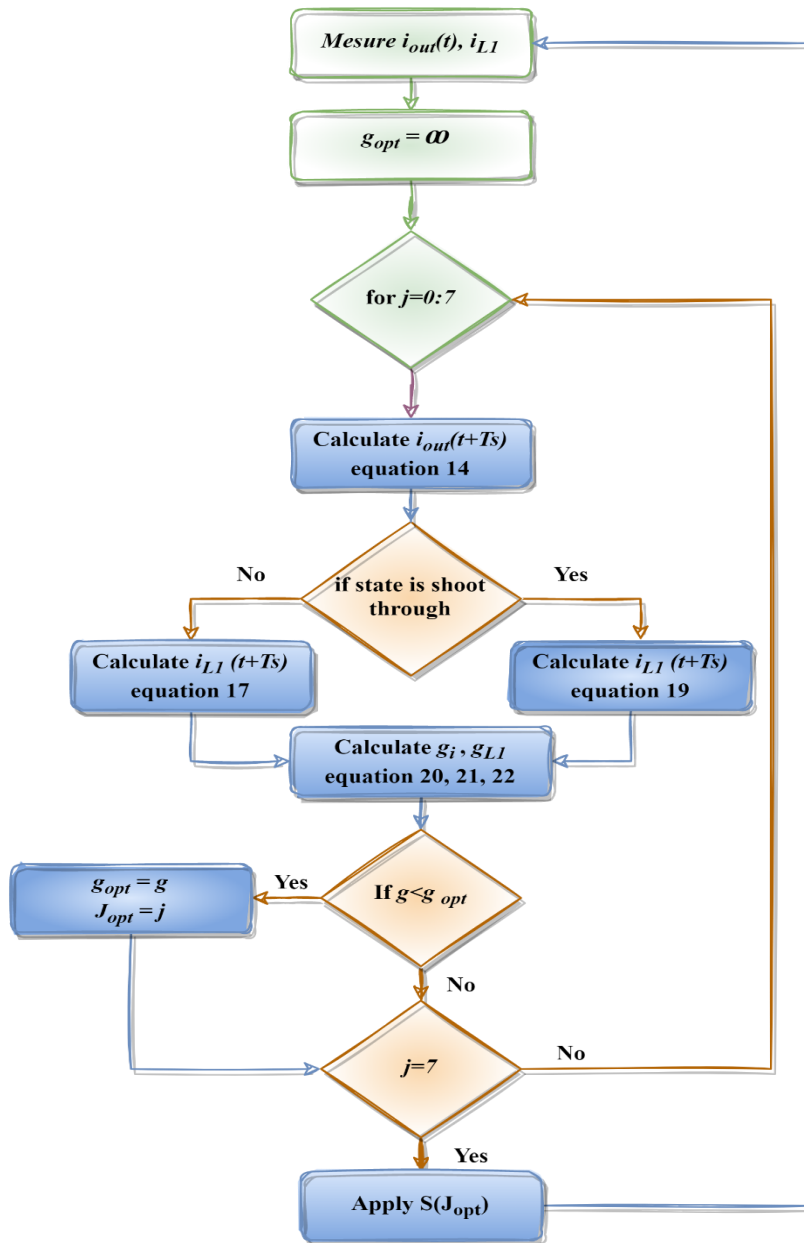


Figure II.11: MPC flowchart for qZSI.

Figure II.11 shows the selection process of the optimal switching states in each sampling period, the first step is to measure the variables $i_{out}(t)$ and $i_{L1}(t)$, then initialize the algorithm by setting the optimal cost function (g_{opt}) to ∞ . After, the algorithm enters the loop. The controller calculates the predictive value of $i_{out}(t + T_s)$ from (14), then check the shoot-through state and calculate the predictive value $i_{L1}(t + T_s)$ from (17) or (19). The controller starts the optimization by calculating the cost function using (22), thus, the selector chooses the optimal switching state, which minimizes the cost function.

II.4. Simulation results

A simulation prototype of a grid-connected PV system based on qZSI has been implemented Matlab/Simulink in order to check the studied algorithms. The system simulation circuit is shown in the Figure II.12. The PV array consists of four PV modules (1Soltech 1STH-215-P) connected in a 2 (series) x 2 (parallel). PV module parameters are shown in Table II.1. Figures II.13 and II.14 illustrate current-voltage (I-V) and power-voltage (P-V) characteristics of the PV module. The system consists also of a qZSI used as boost and conversion stage, a utility grid which is modelled as a sinusoidal voltage source in series with a resistance R and an inductance L, an MPPT control to extract the Maximum power from the PV array, a Proportional- integral (PI) block to control the capacitor C_1 voltage, an MPC bloc to control the inverter. The system contains also current and voltage sensors. The electrical parameters of the grid-connected PV system based on qZSI are listed in Table II.2.

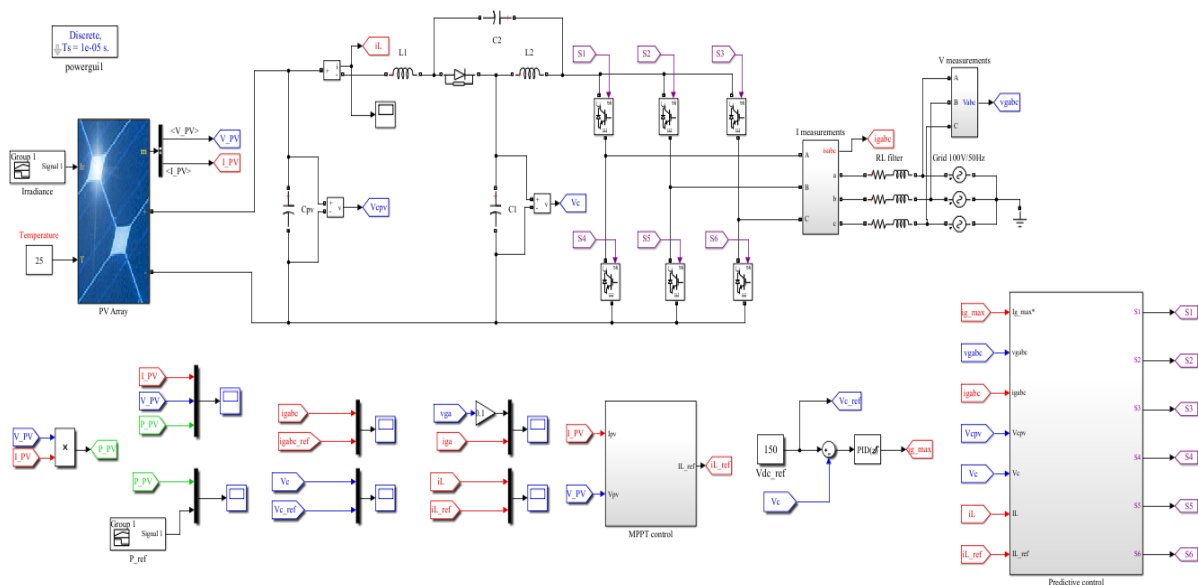


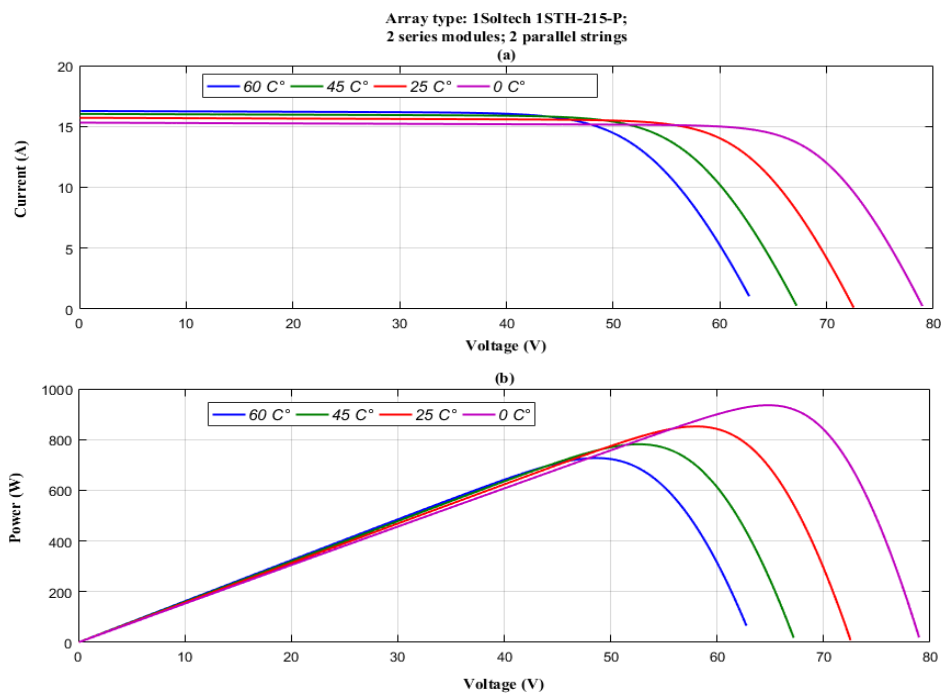
Figure II.12. Schema block diagram of the developed simulation.

Table II.1: PV module parameters.

PV Array	Values
Open circuit voltage (V_{oc})	39 V
Optimum operating voltage (V_{mpp})	36.3 V
Short circuit current (I_{sc})	7.84 A
Optimum operating current (I_{mpp})	7.35 A
Maximum power (P_{mpp})	213.15 W
Temperature coefficient of V_{oc}	-0.36099 %/C°
Temperature coefficient of I_{sc}	0.102 %/C°
Cell per module (N_{cell})	60

Table II.2: Electrical Parameters of the grid-connected PV system.

Component	Nominal value
Capacitance C_1, C_2, C_3	1100e-6 (F)
Resistance R	0.1 Ohm
Inductance L	10e-3 (H)
Voltage source V_a, V_b, V_c	50Hz, 100 (V)

**Figure II.13: Current-voltage (a) and power-voltage (b) characteristics of the PV array for different temperatures.**

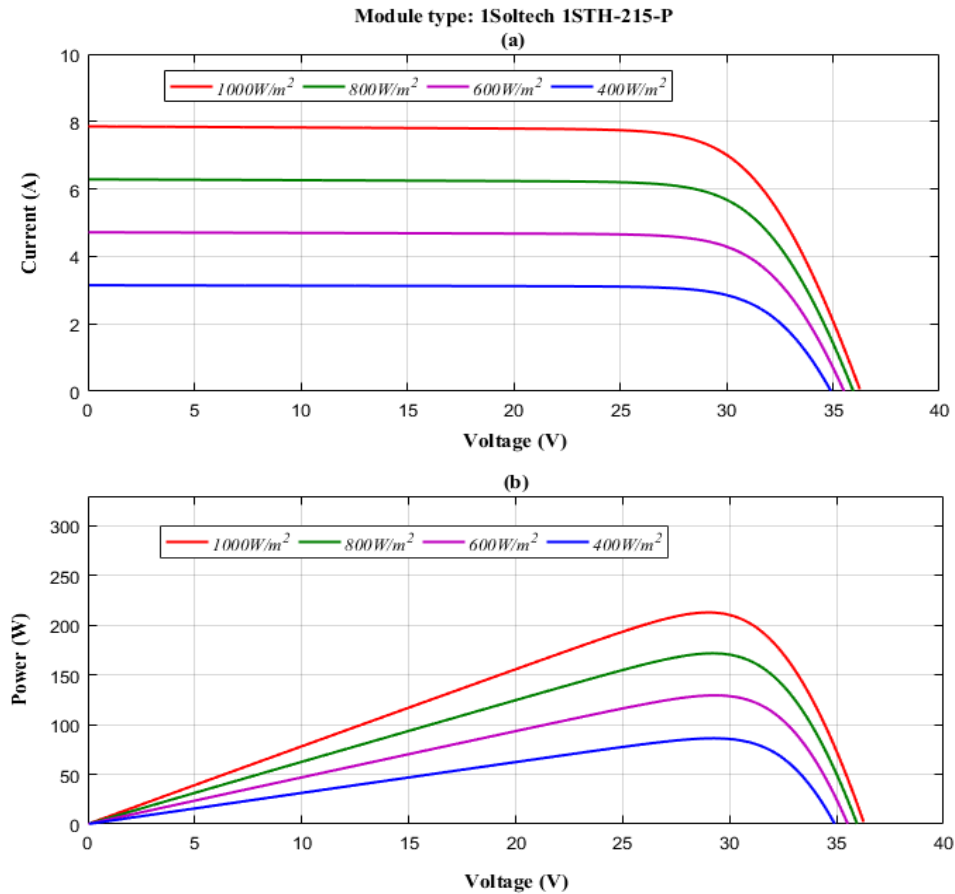


Figure II.14: Current-voltage (a) and power-voltage (b) characteristics of the PV array for different irradiance levels.

Two tests will be done, first when the irradiation is 1000 W/m² during a time period of 1 seconds. For the second test, a climate change is considered to ensure that the system works well in real conditions which means sudden increasing or decreasing in the irradiation. The irradiation is 1000 w/m² at the beginning then decrease suddenly to 800 w/m² in 0.5s, after 0.5s decrease again to 600 w/m² and then increase simultaneously in 1.5s to 900 w/m². The temperature is considered constant (25 C°) in both tests.

❖ **Test 1 : Fixed climatic conditions (G=1000 W/m² and T=25°C)**

The simulation waveforms of PV power, voltage and current obtained from the PV array using the P&O based on MPC algorithm are illustrated in Figure II.15. The irradiance level is set to 1000 W/m² during the simulation, it is observed that the MPP is reached at 0.051s and the PV power is fluctuating around the MPP (848 W–852 W). Figures II.16 and II.17 illustrate waveforms of capacitor C_1 voltage and inductor L_1 current successively. We notice that V_{C1ref} starts to follow the reference voltage ($V_{C1ref} = 150V$) at 0.3s and keep following it till the end, L_1 current also follows the command ($i_{L1reference}$) of P&O algorithm. High frequency

current ripples are due to the inductor L_1 charge in shoot-through state and discharge in non-shoot-through state, the length of shoot-through duty cycle may affect the current ripples.

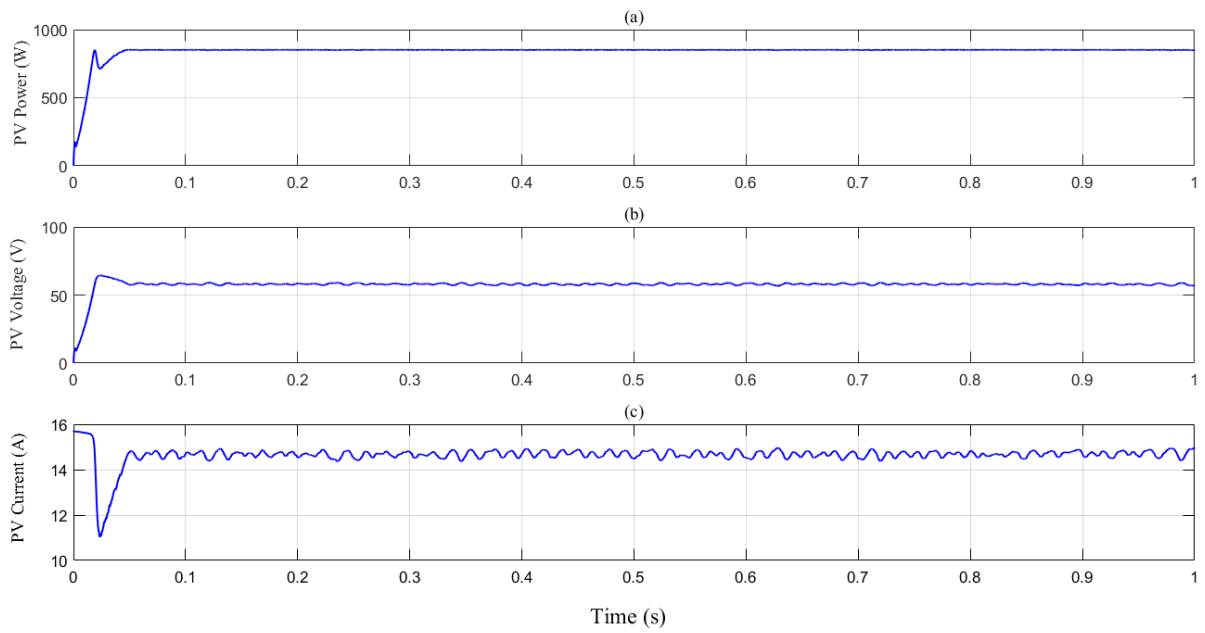


Figure II.15: Waveforms of: (a) PV power, (b) PV voltage and (c) PV current array under fixed climatic conditions.

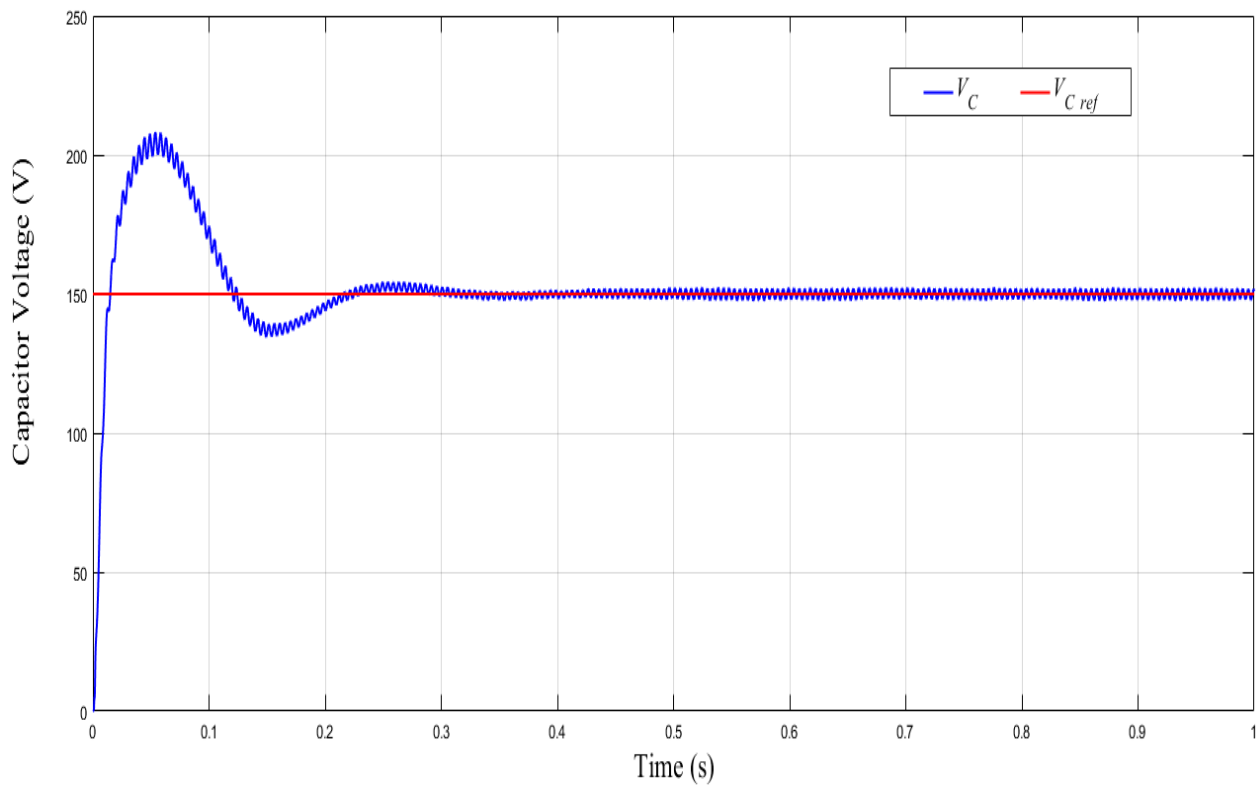


Figure II.16: Waveform of capacitor C_1 voltage under fixed climatic conditions.

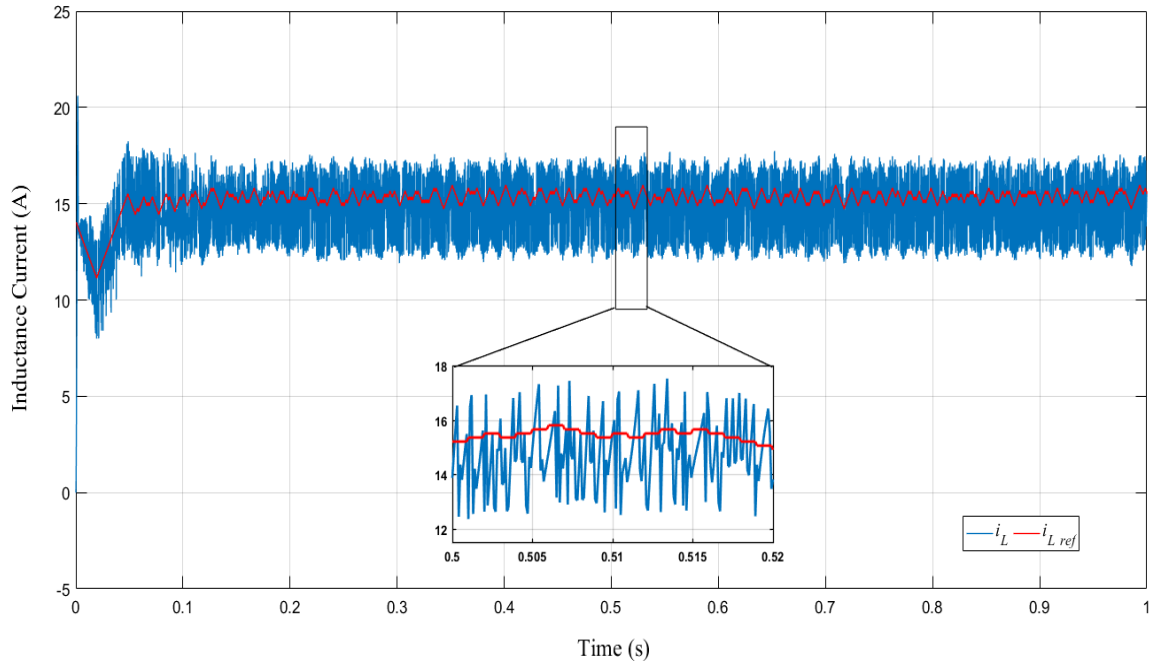


Figure II.17: Waveform of inductor L_1 current under fixed climatic conditions.

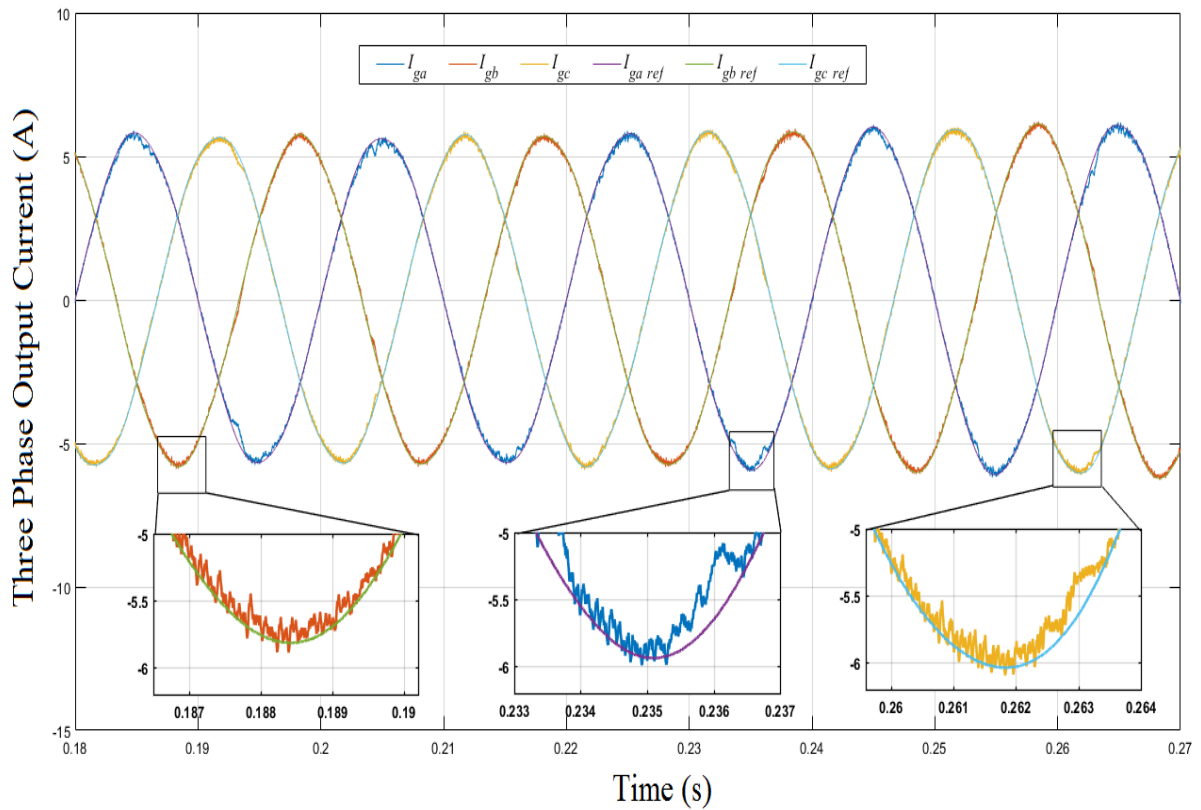


Figure II.18: Waveforms of grid-injected three-phase currents under fixed climatic conditions.

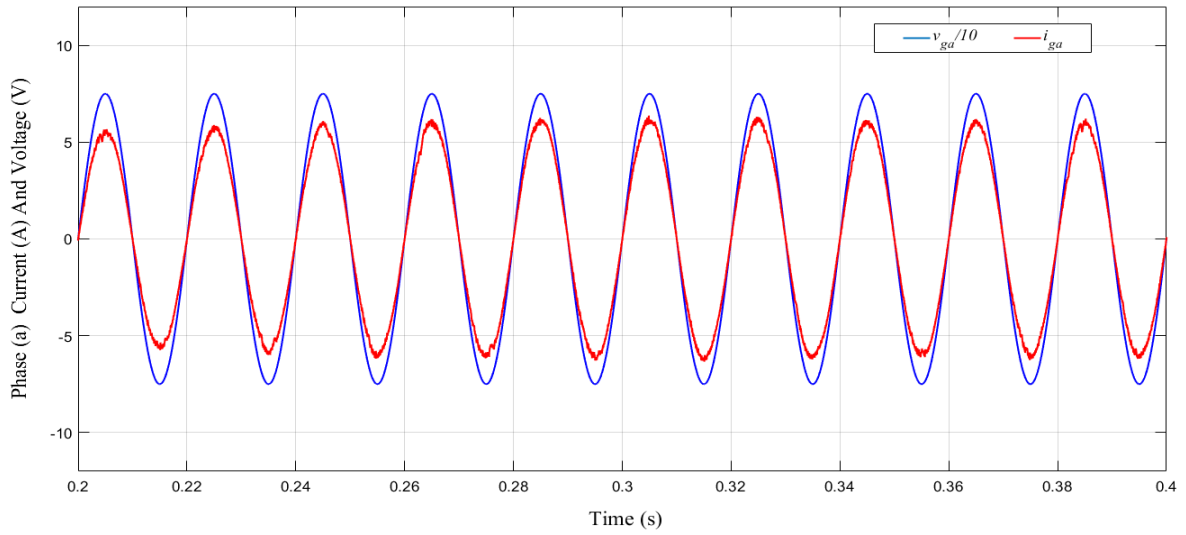


Figure II.19: Grid-injected phase (a) current and voltage (i_{ga} & v_{ga}).

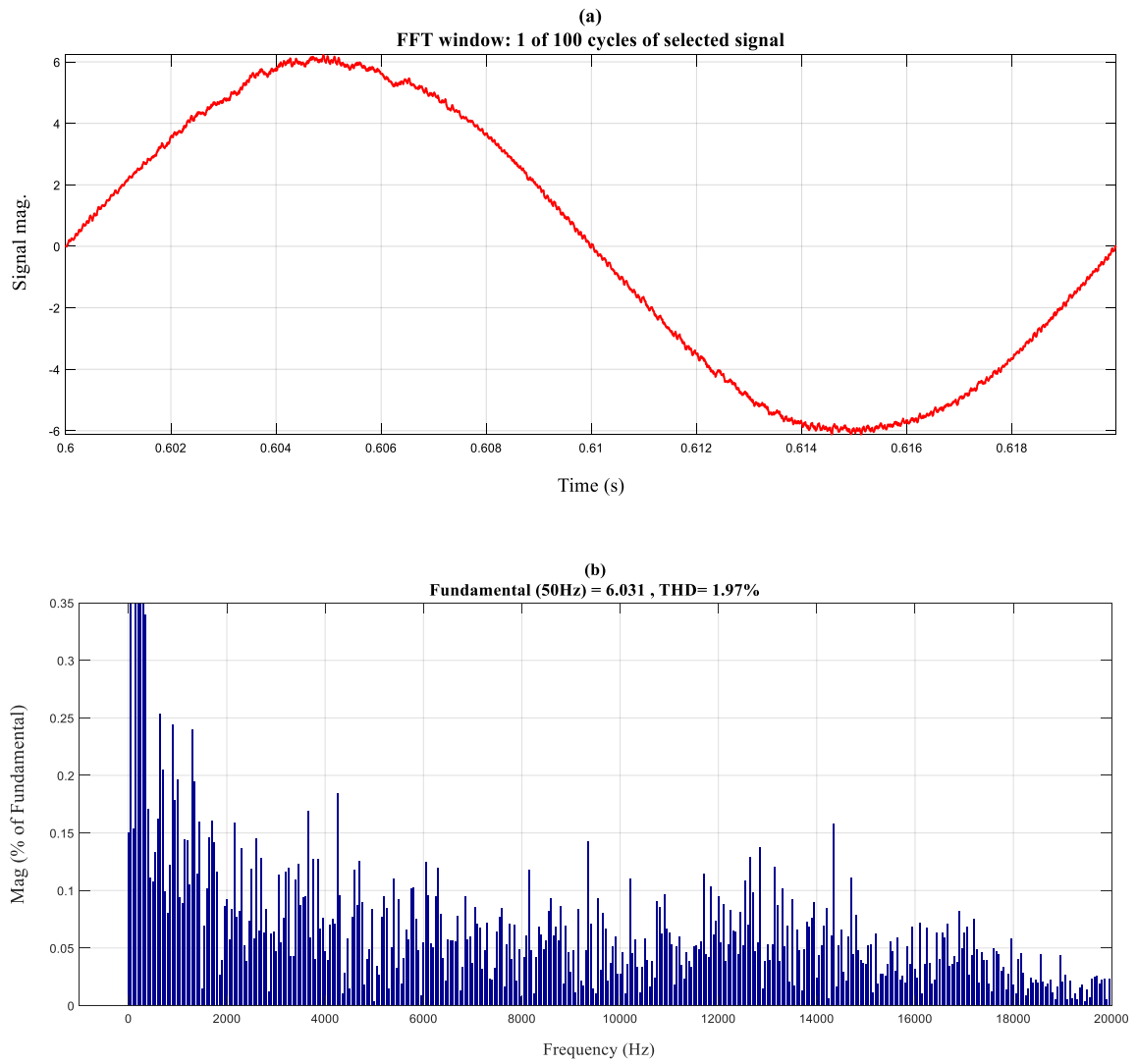


Figure II.20: FFT analysis of phase (a) output current under fixed climatic conditions.

From Figures II.18 and II.19, which present respectively the three-phase qZSI current injected to the grid (i_{gabc}), and the phase (a) current and voltage (i_{ga}, v_{ga}), we observe that the grid currents are in balance, sinusoidal form and strongly follow their references. Furthermore, single phase current i_{ga} is in phase with the voltage v_{ga} , which verifies the unity power factor operation. In addition, we observe from figure II.20 that THD is less than 5% which proves the high grid current quality in case of constant irradiance 1000 W/m^2 regard to the international standards (IEEE-519).

❖ **Test 2 : Sudden changes in the irradiance level**

At the beginning, the irradiance level is set to 1000 W/m^2 , from Figure II.21, which illustrates the PV power during the second test, we observe that the P&O algorithm based on MPC current control reached MPP after 0.051s and the PV power is moving around MPP ($849 \text{ W} - 852 \text{ W}$). A sudden solar irradiance decrease happened at 0.5s from 1000 W/m^2 to 800 W/m^2 , the algorithm needed 0.012s to track the MPP and the PV power oscillation was less than 2 W. After, the irradiance decreased again directly from 800 W/m^2 to 600 W/m^2 at 1s, the MPP is achieved in about 0.014s and the PV power is fluctuating around MPP ($515 \text{ W} - 518 \text{ W}$). The irradiance increased to 900 W/m^2 , the P&O algorithm based on MPC current control tracked the MPP in 0.015 and the PV power oscillate around the MPP ($767.5 \text{ W} - 770 \text{ W}$). The average tracking time for current P&O algorithm based on MPC is 0.0136s.

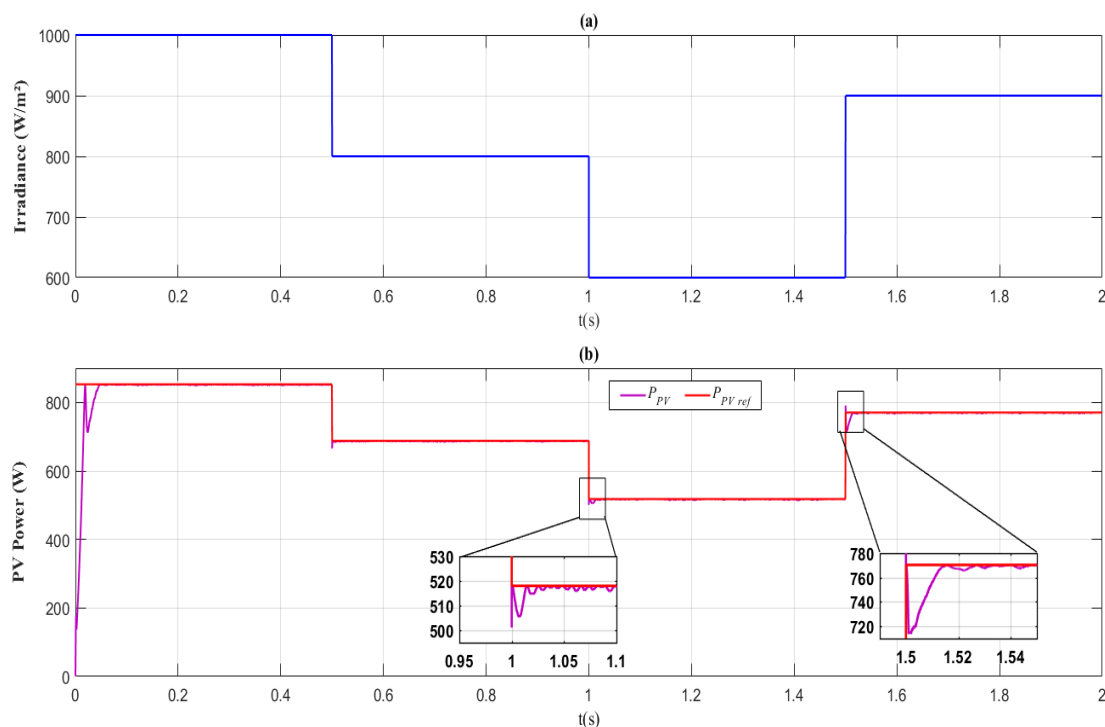


Figure II.21: Waveforms of (a) irradiance profile and (b) PV power array during variation in irradiance level.

Figure II.22 shows the capacitor C_1 voltage while changing the irradiance, we note that the average response time is 0.2s, every irradiation variation corresponds to a small sharp distortion in V_{C1} that means the good performance of the PI controller.

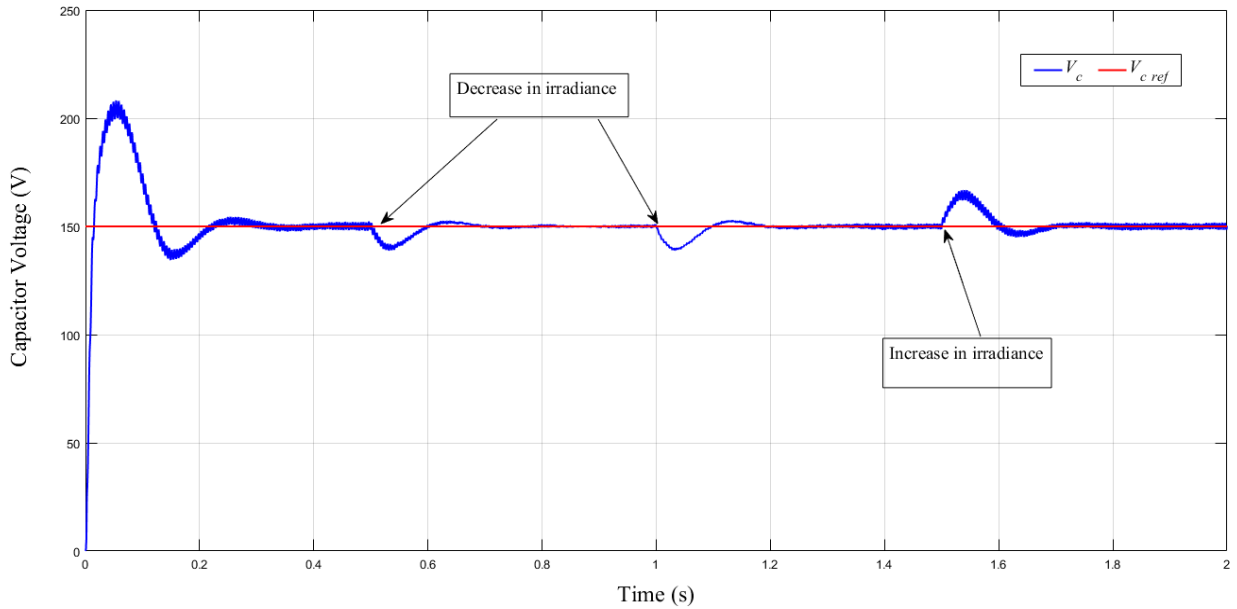


Figure II.22: Waveform of capacitor C_1 voltage during irradiance variation.

Figure II.23 demonstrates the inductor L_1 current waveform $i_{L1}(t)$ during irradiance variation, $i_{L1}(t)$ tracked its reference with high accuracy despite the sudden variation of solar irradiance level, which explains the effectiveness of the used algorithm, high frequency current ripples are because of the inductor L_1 charge and discharge, depending on qZSI operating mode.

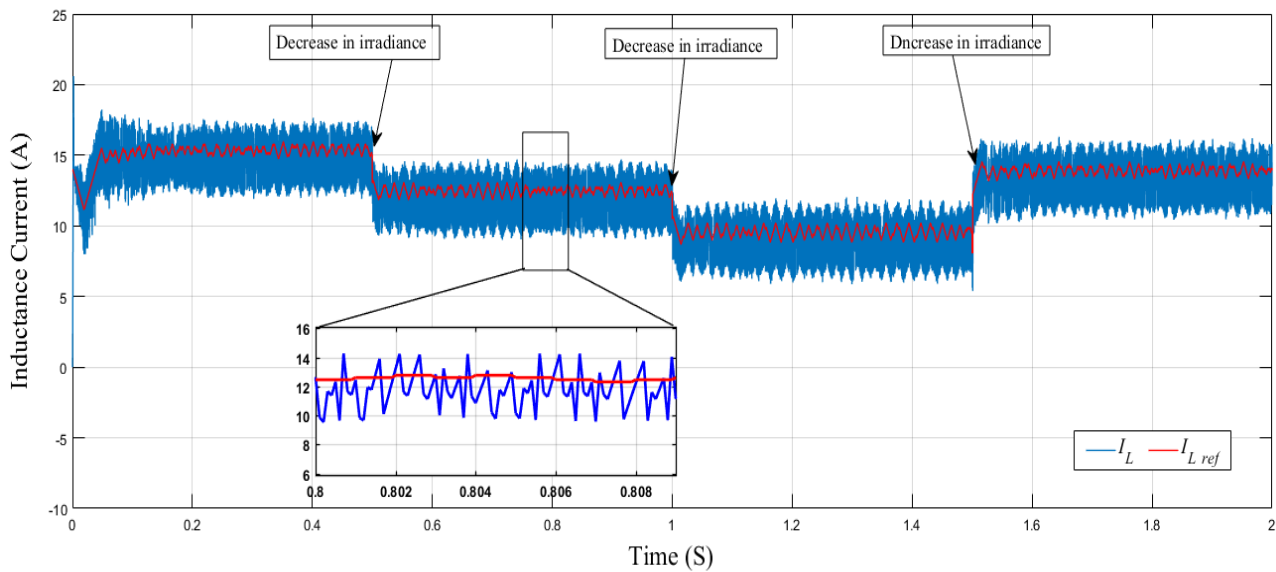


Figure II.23: Waveform of inductor L_1 current during irradiance variation.

As shown in Figure II.24, the grid currents respond to sudden irradiance changes with keeping their sinusoidal forms due to the competence the suggested MPC algorithm.

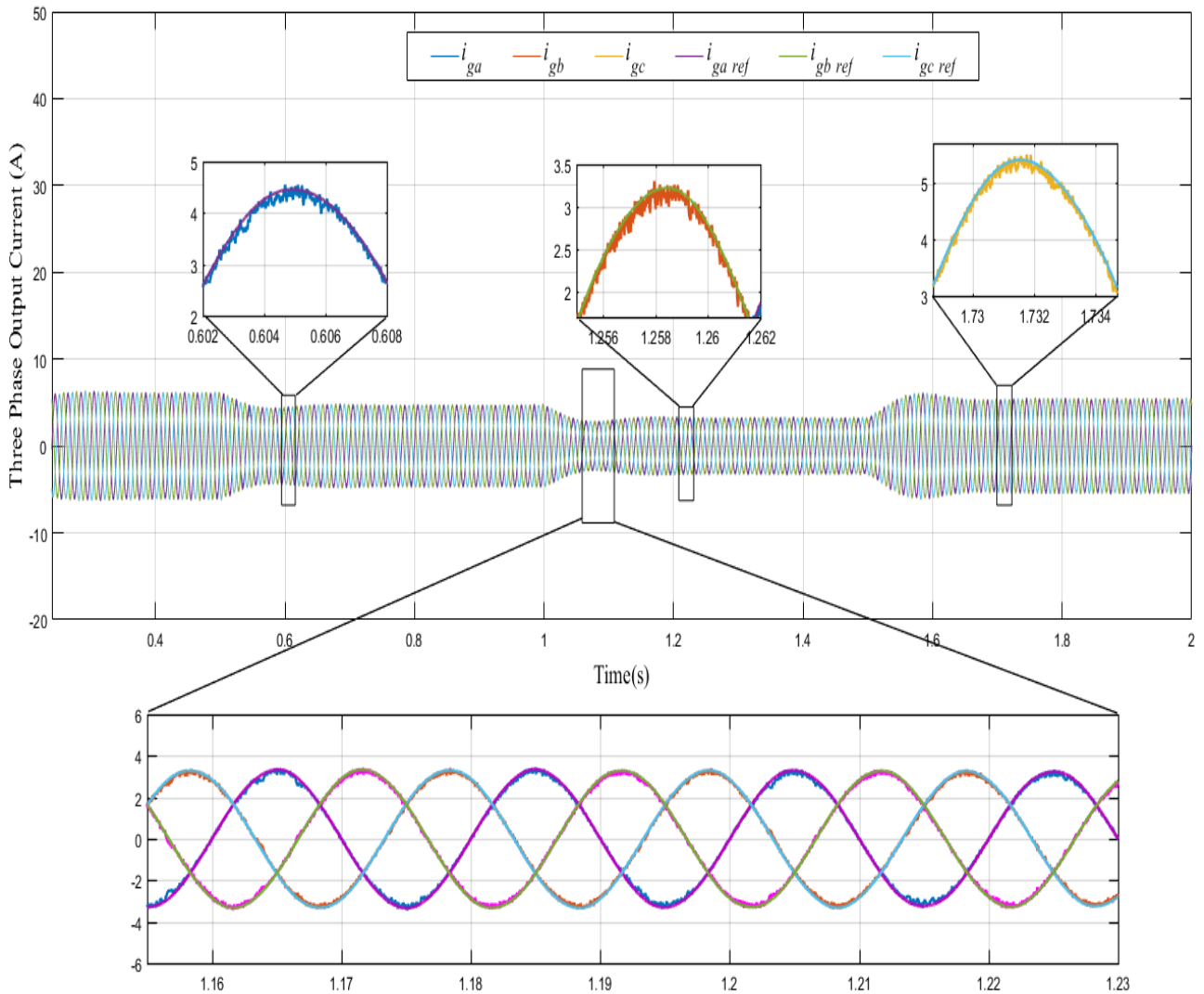


Figure II.24: Waveforms of grid-injected three-phase currents during irradiance variation.

As presented in Table II.3, the suggested control scheme for the single-stage three-phase grid-connected PV system provided high grid current quality under all irradiance change cases regard to the international standards (IEEE-519).

Table II.3: Obtained THD under different irradiance levels.

Irradiance (W/m ²)	600	800	900	1000
THD (%)	3.66	2.46	2.33	1.97

II.5. Conclusion

In this chapter, a control scheme based on model predictive control for three-phase single-stage grid-connected PV system using quasi-Z source inverter is suggested and discussed. The simulation results show a good tracking performance for the maximum power points of the PV array under sudden irradiance changes. Moreover, the studied grid-connected PV system with the suggested MPC algorithm injects the PV power with high grid current quality compare to the international standards (IEEE-519) in different irradiance changes levels.

General Conclusion

This work is a Master's thesis in Electronic Industries carried out at the University Of Mohamed El-Bachir El Ibrahimy on the optimization of the exploitation of the PV energy. The objective of this work is to develop an effective control scheme for a photovoltaic system connected to the utility grid.

In this context, we have presented and modeled a grid-connected PV system, consisting mainly of a PV array and a quasi-Z source inverter (qZSI). The qZSI is a cheap, simple, and a single stage approach for PV arrays. In addition, a control scheme based on model predictive control (MPC) is suggested. The purposes of the suggested controller scheme are :

- Track the maximum power point rapidly and accurately under sudden irradiance changes.
- Control the voltage capacitor of the qZSI at a desired value to assure a proper operation for the inverter.
- Ensure a high quality with a reasonable THD value of the injected currents into the grid.

To show the performance improvement of the suggested control systems, a completed simulation models have developed using MATLAB/Simulink. The obtained results indicated the excellent performance of the proposed control schemes.

Nevertheless, the work presented in this thesis opens up a wide range of perspectives. We can mention the following points:

- Performance test of MPPT controls studied under partial shading conditions.
- Some other MPPT algorithm can be tried and tested.
- Possibility to connect this topology to different other renewable energy sources.

References

- [1] Manisha Joshi. Prof.Dr. Mrs.G.A. Vaidya. Modeling and Simulation of Single-Phase Grid Connected Solar Photovoltaic System. Article. IEEE. INDICON. 2014.
<https://ieeexplore.ieee.org/document/7030623>.
- [2] Bader Nasser Alajm. Design and Control of Photovoltaic Systems in Distributed Generation. Doctoral thesis. University of Strathclyde. 2013.
<https://ethos.bl.uk/OrderDetails.do?uin=uk.bl.ethos.576436>.
- [3] Boualem Boukezata. Etude et commande d'une chaine de conversion d'énergie d'un système solaire photovoltaïque. Doctoral thesis. Ferhat Abbas University. Setif1. Algeria. February 2017.
https://www.theses-algerie.com/6719159326280584/these-de-doctorat/universite-ferhat-abbas-setif-1/etude-et-commande-dune-chaine-de-conversion-denergie-dun-systeme-solaire-photovoltaique?size=n_10_n.
- [4] Frede Blaabjerg. Dan M. Ionel. Renewable Energy Devices and Systems with Simulations in MATLAB ® and ANSYS ®. CRC Press. 2017.
<https://www.routledge.com/Renewable-Energy-Devices-and-Systems-with-Simulations-in-MATLAB-and-ANSYS/Blaabjerg-Ionel/p/book/9780367656218>.
- [5] Bennacer El Hassouni, Ali Haddi. Abdellatif Ghacham Amrani. Modeling and simulation of an autonomous PV Generator dedicated to supply an agricultural pumping station. Article. ICOME 15, 19-22 May 2015, Tetouan, Morocco. ICOME 16, 17-20 May 2016, La Rochelle, France.
<https://reader.elsevier.com/reader/sd/pii/S187661021735600X?token=F6602D382808C18B3349DDE0CD7C398CD4C25FE954CA4C5AE88FDB0906251949F702202A8473CB106A6B29FCDA085851&originRegion=eu-west-1&originCreation=20210902230929>.
- [6] Fang Zheng Peng. Z-Source Inverter, IEEE Trans. Ind. Appl. 39, 504-510, 2003.
<https://ieeexplore.ieee.org/document/1189228>.

- [7] Mostafa Ahmed Mohamed Mosa. Model predictive control technique of multilevel inverter for PV applications. Doctoral thesis, Texas A&M University. May 2018. <https://oaktrust.library.tamu.edu/handle/1969.1/188886>.
- [8] Billel Talbi. Contribution à l'Amélioration de la Commande d'un Système de Pompage Photovoltaïque. Doctoral thesis. Ferhat Abbas University. Setif1. Algeria. June 2018. <https://123dok.net/document/wq2903ez-contribution-l-amelioration-commande-systeme-pompage-photovoltaïque.html>.

Abstract:

This work presents a study of grid-connected PV system using qZ-source inverter. This inverter offer the ability of a booster chopper and an inverter in one conversion stage. In addition, a model predictive control (MPC) method is designed to control the qZ-source inverter by insertion of shoot-through state with the qZ-source network together to achieve a best efficiency and reduce the Total Harmonic Distortion (THD). In addition, the developed control scheme integrated a Perturbation and observation (P&O) MPPT technique to assure the functionality of the photovoltaic generator at the maximum power. The global system is simulated using numerical MATLAB/Simulink software in order to evaluate the suggested control scheme based on MPC. The obtained simulations results show that the grid-connected PV system using qZ-source inverter controlled by the suggested scheme provides high control performance regarding international standards (IEEE-519).

Keywords: qZ-source inverter, photovoltaic generator (GPV), Shoot through State, MPC Control, P&O MPPT technique, Grid.

Résumé :

Ce travail présente une étude d'un onduleur à qZ source connecté à un générateur PV. Cet onduleur assure les deux fonctions d'un hacheur booster et d'un onduleur en un seul étage. En outre, une méthode de contrôle prédictif a été utilisée pour contrôler l'onduleur à qZ source par l'insertion d'un état de court-circuit avec le réseau à qZ source afin d'obtenir le meilleur rendement et de réduire la distorsion harmonique totale (THD). De plus, le schéma de commande développé a intégré une commande MPPT perturbation et observation (P&O) pour obtenir un rendement optimal de la puissance du générateur photovoltaïque (GPV). Le système global est simulé à l'aide du logiciel MATLAB/Simulink afin d'évaluer le schéma de commande suggéré basé sur MPC. Les résultats des simulations obtenues montrent que le système photovoltaïque connecté au réseau à l'aide de l'onduleur à qZ source commandé le schéma suggéré offre des bonnes performances selon les normes internationales (IEEE-519).

Mots clés : onduleur à qZ source, générateur photovoltaïque (GPV), état court-circuit, contrôle MPC, commande MPPT P&O, réseau.

ملخص :

يقدم هذا العمل دراسة لمصدر qZ العاكس المتصل بالمولد الكهروضوئي ، لتحسين أداء العاكس الكلاسيكي. علاوة على ذلك ، يضمن هذا العاكس وظيفة كل من المروحية المعززة والعاكس في مرحلة واحدة. بالإضافة إلى ذلك ، تم استخدام طريقة التحكم التنبؤية النموذجية للتحكم في عاكس مصدر qZ عن طريق إدخال حالة إطلاق النار مع شبكة مصدر qZ معاً لتحقيق أفضل كفاءة وتقليل إجمالي التشوه التوافقي (THD). يتم استخدام تقنية MPPT للحصول على أداء الطاقة الأمثل للمولد الكهروضوئي (GPV). سمحت تقنية MPPT بالحصول على الأداء الأمثل للطاقة للمولد الكهروضوئي (GPV). تم الحصول على نتائج المحاكاة بواسطة MATLAB / Simulink Software العديدة للتحقق من صحة اقتراح الدراسة.

الكلمات الرئيسية: عاكس مصدر qZ ، مولد كهروضوئي (GPV) ، التصوير من خلال الحالة ، تحكم MPC ، تقنية MPPT ، الشبكة.